PHILOSOPHICAL TRANSACTIONS OF THE ROYAL SOCIETY B BIOLOGICAL SCIENCES

Whorl morphogenesis in the dasycladalean algae: the pattern formation viewpoint

Jacques Dumais and Lionel G. Harrison

Phil. Trans. R. Soc. Lond. B 2000 **355**, 281-305
doi: 10.1098/rstb.2000.0565

THE ROYAL SOCIETY

Whorl morphogenesis in the dasycladalean algae: the pattern formation viewpoint

Jacques Dumais[1]† **and Lionel G. Harrison**[2*]

[1]*Department of Botany, University of British Columbia, Vancouver, British Columbia, Canada V6T 1Z4*
[2]*Department of Chemistry, University of British Columbia, Vancouver, British Columbia, Canada V6T 1Z1*

CONTENTS **PAGE**

The dasycladalean algae produce diverse whorled structures, among which the best known are the vegetative and reproductive whorls of *Acetabularia acetabulum*. In this paper, we review the literature pertaining to the origin of these structures. The question is addressed in terms of the necessary pattern-forming events and the possible mechanisms involved, an outlook we call the pattern formation viewpoint. The pattern-forming events involved in the morphogenesis of the vegetative and reproductive whorls of *Acetabularia* have been used to define five and six morphogenetic stages, respectively. We discuss three published mechanisms which account, at least in part, for the pattern-forming events. The mechanisms are mechanical buckling of the cell wall, reaction–diffusion of morphogen molecules along the cell membrane, and mechanochemical interactions between Ca^{2+} ions and the cytoskeleton in the cytosol. The numerous differences between these mechanisms provide experimental grounds to test their validity. To date, the results of these experiments point towards reaction–diffusion as the most likely patterning mechanism. Finally, we consider the evolutionary origin of the vegetative and reproductive whorls and provide mechanistic explanations for some of the major evolutionary advances.

Keywords: *Acetabularia*; whorl morphogenesis; morphogenetic models; Dasycladales; spacing; evolution

1. INTRODUCTION

The order Dasycladales comprises 11 extant genera of unicellular green algae inhabiting shallow, protected waters of warm seas. All species elongate by tip growth forming, at regular intervals, whorls of branching appendages. Differentiation of these whorls is under the control of a single nucleus located in the anchoring basal part, the rhizoid. Development of the dasycladalean algae has been studied repeatedly since Nägeli's descriptive work (Nägeli 1847) and particularly since the genus

*Author for correspondence (lionel@pepe.chem.ubc.ca).
† Present address: Department of Biological Sciences, Stanford University, Stanford, CA 94305, USA.

Received 10 February 1999 *Accepted* 25 May 1999

Acetabularia was introduced to cell biology by Joachim Hämmerling (1931). Their unicellular state, complex morphology and extensive fossil record are all attractive features to the student of morphogenesis.

Recent reviews have addressed dasycladalean development from a variety of standpoints: Vanden Driessche *et al*. (1997) reviewed the cell biology, Mandoli (1996) covered the genetic control of development, and Menzel (1994) emphasized the role of the cytoskeleton. Here we review a complementary body of literature and provide a perspective that has so far been neglected (see below). Previously unreported work of our own is also included and identified as such.

(a) *The pattern-formation viewpoint*

It is paradoxical that developmental studies of the Dasycladales have mostly emphasized fully developed structures rather than the various stages of development. Valet (1968) and Werz (1965) must be credited for the first definite attempts to study development as it unfolds. With this approach, Valet was able to present a precise morphogenetic sequence for several dasycladalean species. We believe that to understand morphogenesis one must first establish such a morphogenetic sequence by identifying individual pattern-forming events leading to the final morphology. The next step is to determine the mechanism controlling each pattern-forming event. We call the practice of identifying pattern-forming events and looking for their mechanisms the 'pattern-formation viewpoint'. Our review of dasycladalean development is based on that perspective.

(b) *Life cycle of* Acetabularia

The life cycle of *Acetabularia acetabulum* (L.) Silva may span two or three years in the natural habitat (Woronine 1862; de Bary & Strasburger 1877) but is reduced to approximately six months in culture and can be shortened to three or four months under especially favourable conditions (Zeller & Mandoli 1993). The full cycle consists of three main differentiation processes: cell differentiation, cyst differentiation, and gamete differentiation (figure 1; Bonotto & Kirchmann 1970). Cell differentiation begins with the fusion of two isogametes to form the zygote. The zygote then differentiates into a rhizoid, a stalk, numerous vegetative whorls (hair whorls) and a terminal reproductive whorl (cap). Hair whorls contribute to the photosynthesis and nutrient uptake (Gibor 1973) necessary for vegetative growth but are shed approximately two weeks after their initiation. The cap forms just prior to reproduction. When it is fully developed, the single nucleus located in the rhizoid undergoes meiosis and numerous rounds of mitosis to give around 10^4 secondary nuclei (Schweiger *et al*. 1974; Nishimura & Mandoli 1992*b*). These then migrate to the gametophores (cap rays). During cyst differentiation, the cytoplasm inside the gametophores is partitioned around each secondary nucleus and a cell wall is formed. Gamete differentiation takes place within each cyst, the secondary nucleus dividing usually ten times to yield around 10^3 gametes (Schweiger *et al*. 1974). The life cycle is completed when the operculum of the mature cyst opens, liberating the biflagellate gametes for mating. Cell differentiation can be further divided into developmental phases (figure 1; Nishimura & Mandoli 1992*a*; Mandoli 1998). These phases (zygotic, juvenile, adult and reproductive) resemble those characterizing higher plant development (see, for example, Poethig 1990). This review focuses on whorl formation during cell differentiation. The reader is referred to the literature for descriptions of cyst differentiation (Werz 1968; Menzel & Elsner-Menzel 1989, 1990), gametogenesis (Dao 1957) and zygote differentiation (Crawley 1966; Kellner & Werz 1969; Berger & Kaever 1992). Alternative modes of reproduction (e.g. by zoospores or cyst germination) have been described by Puiseux-Dao (1972) and Bonotto (1988, 1994).

2. MORPHOGENETIC STAGING

The adult morphology of most dasycladalean species has been described numerous times (see for example Berger & Kaever 1992) but a definite morphogenetic perspective has been taken in fewer instances. In this section, we present a detailed description of whorl formation in *Acetabularia*, a comparison with selected genera, and a discussion of the variability (or regularity) of some important features. Most of the observations presented here are not new; however, we provide the first explicit staging of whorl formation and illustrations of the critical stages. Our description is based on the observation of cell wall ghosts under a standard compound microscope. These wall ghosts were prepared from free-hand sections and cleaned of their cytoplasmic content with a bleach solution. When needed, the cell wall was stained with toluidine blue.

(a) *Whorl formation in* Acetabularia

The overall appearance of the hair whorl and cap is seen in figure 1, but we also encourage the reader to consult the beautiful monograph by Berger & Kaever (1992). The most complete accounts of whorl formation in *Acetabularia* were provided by Solms-Laubach (1895), Howe (1901) and Valet (1968). We describe the process as a sequence of morphogenetic stages. In this sequence, the transition from one stage to the next involves a pattern-forming event. Consequently, each stage is qualitatively different from the preceding and following stages. Despite their distinct external aspects, the vegetative and reproductive whorls share the same five stages; the cap involves an additional sixth stage (figure 2; abbreviations for this and other figures are given in table 1). Our observations from three *A. acetabulum* cell lines and the descriptions found in the literature suggest that the stages listed below are generally conserved even if differences in final morphology are observed. Because the method employed to analyse whorl formation is destructive, a precise timing of the different stages is still missing. The best assessments to date indicate that the sequence of events depicted in figure 2 requires approximately 15 h for the vegetative whorl (Schmid *et al*. 1987; Harrison *et al*. 1984) and 34 h for the reproductive whorl (Kratz *et al*. 1998). For an alternative staging of cap morphogenesis based on gross morphology see the paper by Kratz and co-workers (1998).

(i) *Stage 1: apical growth*

Apical growth dominates the morphogenesis of *Acetabularia* from the first appearance of polarity in the zygote to

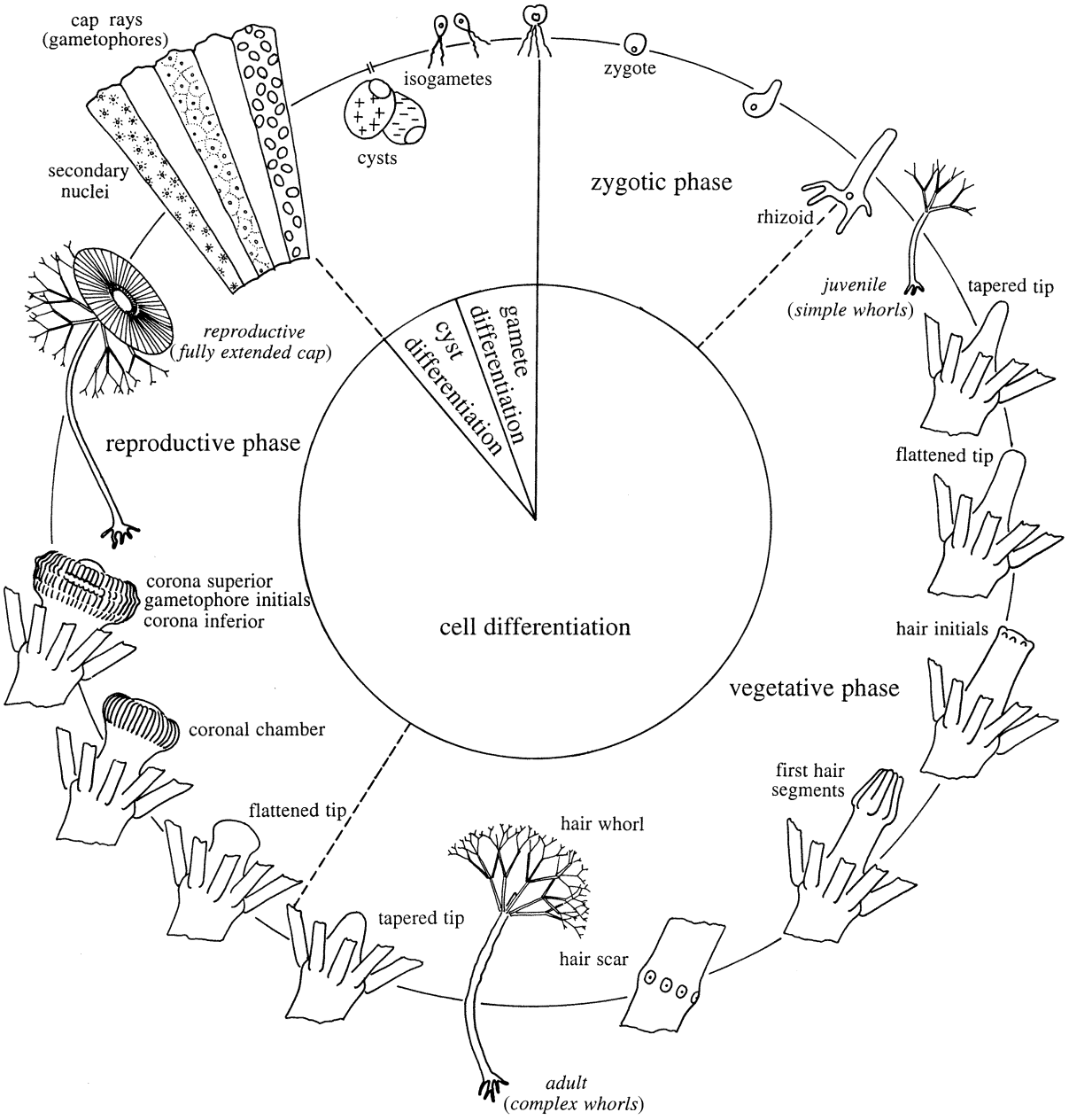

Figure 1. Life cycle of *A. acetabulum*. Inner circle, differentiation processes (Bonotto & Kirchmann 1970); outer circle, developmental phases (Nishimura & Mandoli 1992*a*). In culture, the full cycle is completed in approximately six months. The space allotted in the diagram is proportional to the time spent in each developmental phase (based on Nishimura & Mandoli 1992*a*). During cell differentiation 15 to 20 hair whorls are formed and shed. A single cap is produced at the end of the phase. A detailed staging of whorl formation is presented in figure 2.

the growth of the cap. When wall extension is isotropic, sustained apical growth involves a graded growth rate with a maximum at the pole of the dome and zero growth at the equator (subapical region). The equatorial region must also move along with the tip. Actively growing tips usually have a tapered shape. Apical growth in *Acetabularia* shares features common with tip growing cells such as pollen tubes, fungal hyphae and root hairs (Sievers & Schnepf 1981). For example, the growing apex is densely filled with secretory vesicles (Schmid *et al.* 1987) and Ca^{2+} gradients are observed (Reiss & Herth 1979; Harrison *et al.* 1988). Apical growth is stopped periodically to give place to the whorl-forming stages of morphogenesis (stage 2 and beyond). For cells grown in red light, the transition from apical growth to the following stages is triggered by a flash of blue light (Schmid *et al.* 1987).

(ii) *Stage 2: subapical growth*

A flattening tip is the first morphological indication of whorl initiation. The pattern-forming event involves a redistribution of growth from the apex to a subapical annulus. The lateral bulging of the subapical region is minimal when a vegetative whorl is initiated, but a strong lateral ridge is sometimes seen for the reproductive whorl (compare figures 3*b* and 4*c*). In the latter case, the growing annular region also shows a local wall thickening (figure 4*a*,*b*). The origin and potential role of this thickening are still unknown.

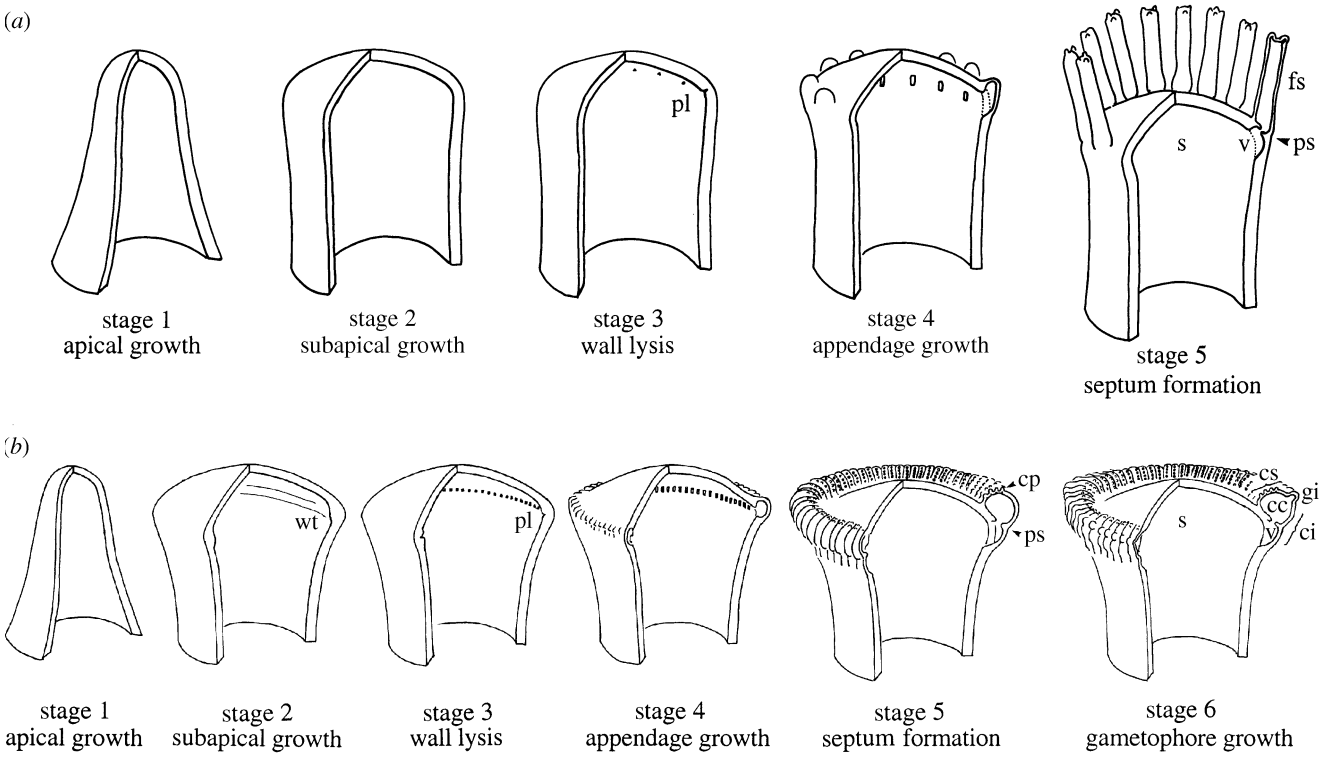

Figure 2. Morphogenetic staging of (*a*) the vegetative and (*b*) the reproductive whorls of *A. acetabulum*. For abbreviations, see table 1.

(iii) *Stage 3: wall lysis*

While the tip is still broadening, a punctate lysis of the inner wall provides the first structural evidence for the location of the whorl appendages (figures 3*a* and 4*c*,*d*). A new pattern-forming event accounts for the transition from the presumably uniform annular region of stage 2 to the whorl pre-pattern of this stage. Werz (1965) published evidence for the nature of the lysis process. First, uncharacterized proteins accumulate in the morphogenetic region and indicate the future location of the appendages. Second, a close association between the endoplasmic reticulum and the lysis sites is seen, suggesting that local secretion of hydrolytic enzymes is responsible for the wall lysis. At the inception of lysis, the pattern is constrained to a narrow line circling the broadened tip. In the vegetative whorl, this lysis pattern is established at the periphery of a flat region and is more distinctly seen from above (figure 3*a*,*b*). In the reproductive whorl, the lysis pattern emerges laterally, precisely in the region of greatest curvature (figure 4*c*,*d*). In both cases, the lysis sites start as very fine notches in the inner wall. Later, these notches extend along the cell axis to form small chambers in the cell wall (figure 4*e*,*f*). The spacing (λ) between successive lysis sites is 4–5 µm in the cap and 5–10 µm in the hair whorl. The tip diameter at this stage is *ca.* 100–140 µm for the cap and 15–90 µm for the hair whorl. Consequently, the number of lysis sites that can be placed around the tip periphery is large (60–90) for the cap and smaller as well as quite variable (4–35) for the hair whorl. The spacing and tip diameter increase during further development of the whorl but the number of lysis sites, which eventually determines the number of lateral appendages, remains fixed.

(iv) *Stage 4: appendage growth*

As the lysis chambers develop in the cell wall, little bulges reveal their presence externally (figures 3*c*,*d* and 4*e*,*f*). The bulges assume different shapes depending on the type of whorl being produced (vegetative or reproductive). Despite this difference, they go through the same steps of differentiation (i.e. elongation, septum formation and branching). In the vegetative whorl, the transition from wall lysis to the sustained elongation of the appendages requires the establishment of a growth pattern similar to that described for stage 1. For the reproductive whorl, growth is less sharply concentrated at the appendage's apex. This provides for shorter and broader appendages (compare figures 3*e*,*f*,*g* and 4*g*).

(v) *Stage 5: septum formation*

Concurrent with the growth of the appendage, a perforated septum forms slightly distal to the junction between the appendage and the central cavity. This septum divides the appendage into a proximal chamber, the vestibule, and a distal chamber, called the hair segment for the vegetative whorl and the coronal chamber for the reproductive whorl (figures 2, 3*e*,*f* and 4*g*). In contrast to the cap vestibule, which remains visible in the fully grown cap, the hair vestibule is for the most part obliterated during development of the whorl (Valet 1968). The cytoplasmic processes leading to septum formation have not been studied in *Acetabularia*, but the resemblance to the dolipore septum found in Basidiomycetes is striking (see, for example, Orlovich & Ashford 1994; Lü & McLaughlin 1991). Our observations suggest that septum formation involves secretion of new wall material (figure 3*e*) and infurrowing of the lateral wall (figure 4*g*). Externally, the

Table 1. *Abbreviations used in figures*

cc	coronal chamber
ci	corona inferior
cp	corona protuberance
cs	corona superior
fs	first hair segment
g	gametophore
gi	gametophore initial
pl	punctate lysis
ps	perforated septum
s	stalk
ss	second hair segment
v	vestibule
wt	wall thickening

infurrowing leads to the characteristic crease of the corona inferior and a slight girdle-like effect at the base of the hair (figures 3*f*,*g* and 4*g*,*h*). One septal pore allows cytoplasmic communication between the central cavity and the lateral appendage (figures 3*h*,*i* and 4*h*). When the appendage has served its function, or in response to wounding, the cell secretes a plug that closes the pore (Menzel 1980).

Appendages branch soon after septum initiation. The branching process recapitulates stage 1 to stage 5 (for the vegetative whorl see figure 3*f*,*g* and Puiseux-Dao (1965)). In *Acetabularia*, the vegetative hairs branch in this way four to five times, the number of branches formed being reduced each time (Nishimura & Mandoli 1992*a*). The coronal chamber also branches to form the coronal protuberances (figure 4*g*,*h*). These protuberances grow into structures morphologically identical to the vegetative hairs. However, their growth is often delayed or simply arrested. For both the vegetative hair and the coronal chamber, growth is determinate since it stops once the appendage has branched a fixed number of times.

The vegetative and reproductive whorls seem to differ with respect to the branching pattern of their primary segments. In the vegetative whorl, the second-order branches form a whorled pattern, while in the cap the second-order branches (coronal protuberances) are aligned on radial lines (figures 2 and 4*g*,*h* convey in part this impression, but see also Berger & Kaever (1992)). Evidence suggests that the difference is only superficial. Howe (1901) and Valet (1968) observed that the coronal protuberances in *A. acetabulum* are initiated in a whorled pattern, but are soon rearranged in a linear pattern. The extensive radial growth of the coronal chamber which supports the protuberances is probably the direct cause of the rearrangement. We have not been able to confirm or refute this; however, the presence of whorled coronal protuberances in related species such as *A. caliculus* brings additional support to Howe and Valet's observations.

(vi) *Stage 6: gametophore growth*

The growth of the gametophores (i.e. the cap rays where the cysts are formed) is the last morphogenetic stage and pertains to the cap only. The gametophores are initiated on the side of the coronal chambers soon after the emergence of the coronal protuberances (figure 4*g*). Their position delimits the two regions of the coronal chambers: the corona superior and the corona inferior. During the ensuing growth, the gametophore acquires a characteristic club shape and the morphology of the coronal chamber is altered by the appearance of a radial projection above and below the gametophore (compare figure 4*g* and *h*). Contrary to what is seen in the hair, growth is localized at the base of the gametophore rather than at its tip (Serikawa & Mandoli 1998). Moreover, the gametophore lacks the perforated septum.

The lateral appendages, as a whole, differ from the stalk with respect to their mode of branching. First, whorl formation along the main axis occurs at irregular time intervals while the formation of higher-order whorls on the lateral appendages is precisely timed. Second, the segments of lateral appendages do not resume tip growth once they have branched (sympodial branching). The main stalk is capable of resuming growth, allowing for the production of numerous whorls along a single axis (monopodial branching). The re-establishment of apical growth after whorl formation thus represents an additional pattern-forming event for the stalk. The two-stage model presented in § 3(b) provides a mechanistic explanation for the presence of monopodial and sympodial branching (Dumais 1996).

(b) *Whorl formation in other genera*

The morphogenesis of vegetative whorls is essentially the same in all genera, and the description provided for *Acetabularia* is to be used as a reference. The elaboration of reproductive structures shows greater intergeneric variability, and thus deserves further consideration. We have restricted our attention to genera that were available to us (*Polyphysa* and *Batophora*) and to those for which the morphogenesis is adequately described in the literature (*Neomeris* and *Halicoryne*). This is not a great limitation because these genera, along with *Acetabularia*, practically cover the whole range of morphogenesis in the Dasycladales.

(i) Polyphysa peniculus

The morphogenesis of the reproductive whorl in *Polyphysa peniculus* involves the same stages as those previously described for *A. acetabulum* (figure 5). The tip diameter at early stage 4 is between 150 and 200 µm for both genera. However, the cap of *P. peniculus* contains 10–15 appendages rather than the 60–90 appendages seen in *A. acetabulum*. The difference, therefore, corresponds to a much larger spacing (λ) between appendages in *P. peniculus* (at early stage 4, $\lambda \approx 42$ µm for *P. peniculus* and $\lambda \approx 7$ µm for *A. acetabulum*). The cap of *P. peniculus* has additional distinctive features, such as cylindrically shaped coronal chambers (i.e. without radial projections) and coronal protuberances arranged in a whorled pattern. That is, the coronal chambers are much less extended radially in *P. peniculus* than in *A. acetabulum*. They thus resemble short hair segments.

Since the two species share the same morphogenetic stages, an explanation for the differences in coronal morphology must be found elsewhere. We may inquire whether the morphological differences require a precise control mechanism, or whether they are secondary characters not under direct cellular control. We propose that in *A. acetabulum*, the small spacing λ is the source of lateral interference which may perhaps be quantified by

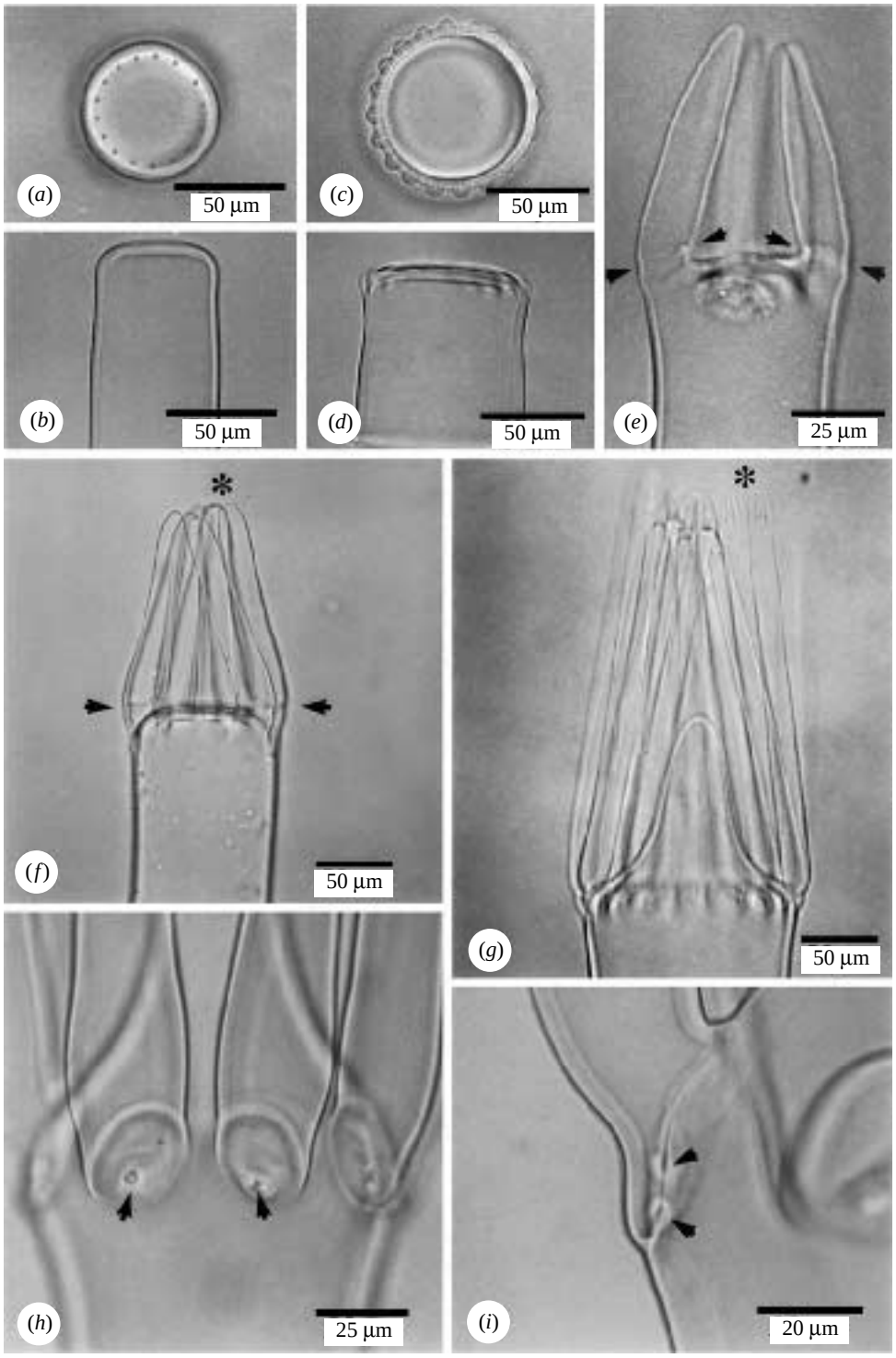

Figure 3. Critical steps in the morphogenesis of the vegetative whorl of *A. acetabulum*. (*a*, *b*) End-on view and optic section of a cell at the wall lysis stage (stage 3). Sixteen evenly spaced lysis sites are visible inside the tip periphery (*a*). The optic section shows the flattened tip and the wall thickness (*b*). (*c*, *d*) End-on view and optic section of a cell at an early stage of appendage growth (early stage 4). Twenty hair initials are visible (*c*). Note the gradation of initial size. (*e*) Septum formation in a small hair whorl (arrows). (*f*) Initiation of secondary branches (asterisk). Note the girdle-like effect at the level where the septum is forming (arrows). (*g*) Growth of the secondary branches. Observe the similarity between whorl formation on primary hair segments (asterisk) and the initiation of a small hair whorl on the stalk (panel *e*). The stalk has resumed apical growth (stage 1). (*h*, *i*) Perforated septa of *Batophora oerstedi*. The pores are visible (*h*, arrows). The thickened lips of the pore can be seen in an optic section (*i*, arrows). Similar septa are found in *Acetabularia*. (Photographs from Dumais 1996.)

the reciprocal of spacing ($1/\lambda$). In other words, the small spacing would constraint the coronal chambers to grow in the radial direction (i.e. away from the cell axis). This would give rise to radial extension of the coronae inferior and superior simply as a result of mechanical forces between adjacent coronal chambers. The fully grown cap would then have radially elongated coronal chambers with the coronal protuberances placed on radial lines.

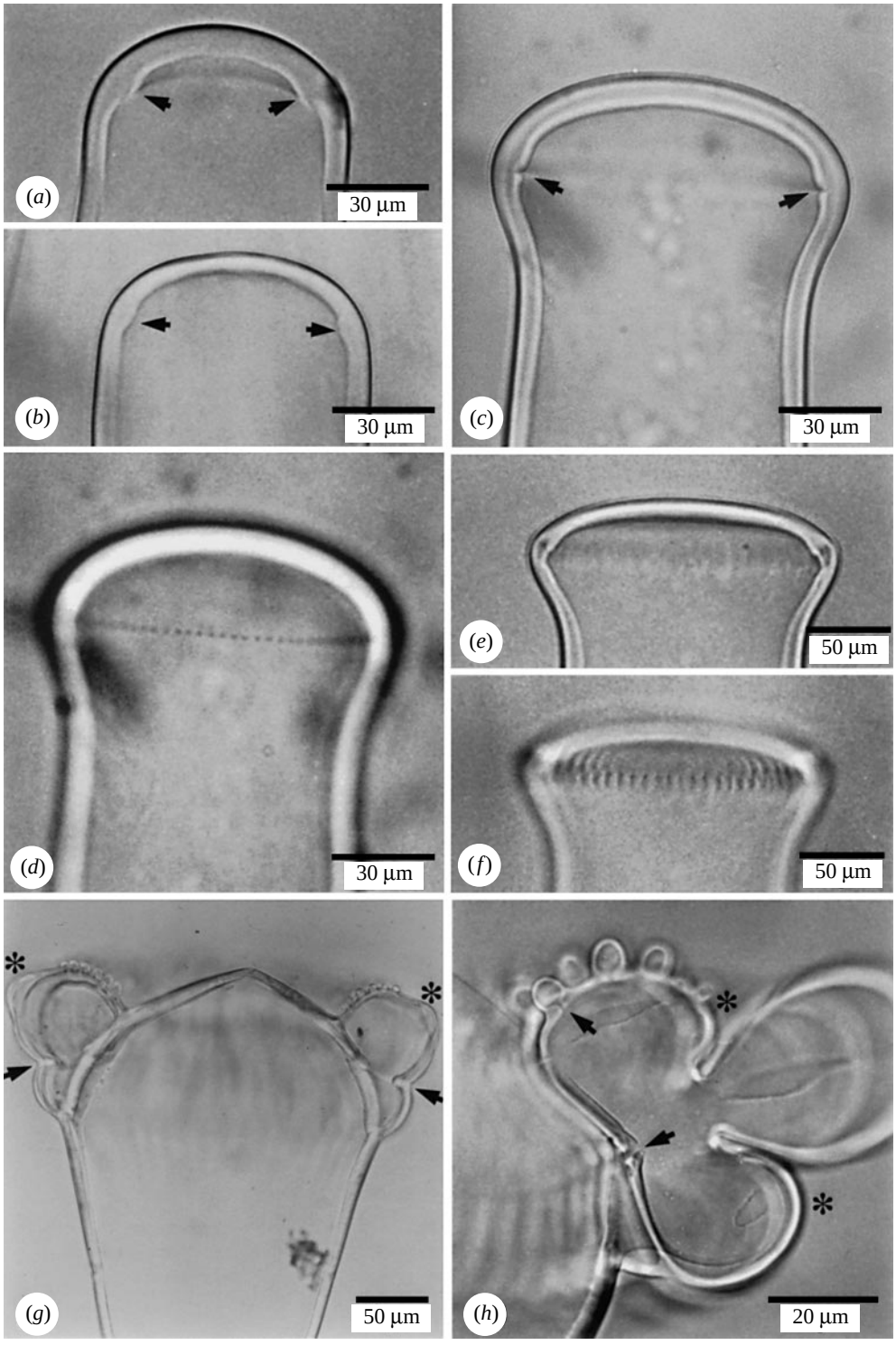

Figure 4. Critical steps in the morphogenesis of the reproductive whorl of *A. acetabulum*. (*a*, *b*) Optic sections of stage 2 cells showing the thickening of the inner wall in the morphogenetic region (arrows). (*c*, *d*) Optic section and surface view of a stage 3 cell showing the lysis of the inner wall (*c*, arrows) and the beautifully regulated spacing (*d*). (*e*, *f*) Optic section and surface view of an early stage 4 cell showing the lysis chambers (*e*) and the bulges that reveal their presence externally (*f*). (*g*) Cross-section of an early stage 6 cell showing two coronal chambers with several protuberances and a gametophore initial (asterisks). Note the crease produced by the perforated septa (arrows). (*h*) Cross-section of a stage 6 cell. The pores leading to the coronal chamber and one of its protuberances are visible (arrows). The radial projections from the coronae inferior and superior are visible above and below the gametophore (asterisks). (Photographs from Dumais 1996.)

Without this spatial constraint, the cap of *P. peniculus* develops like the vegetative whorl where lateral interference is minimal (i.e. the spacing is large).

Evidence that lateral interference is in part responsible for the differences between *Acetabularia* and *Polyphysa* is abundant. First, the correlation between lateral interference and coronal morphology observed for *A. acetabulum* and *P. peniculus* can be extended to other *Acetabularia* and *Polyphysa* species. *Polyphysa* species usually have few cap appendages (10–20) and cylindrical coronal chambers

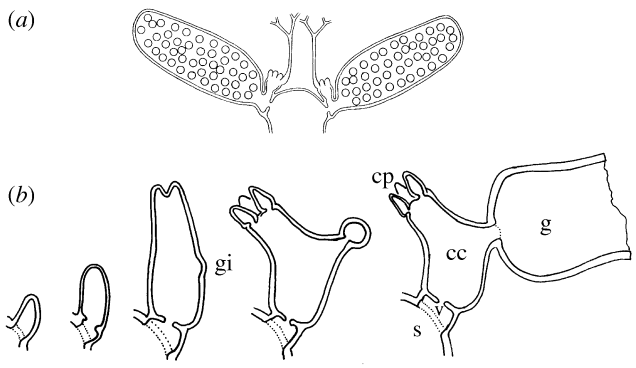

Figure 5. Morphogenesis of the reproductive whorl of *Polyphysa peniculus*. (*a*) Fully developed reproductive whorl (from Berger & Kaever (1992), with permission). (*b*) Morphogenetic sequence. For abbreviations, see table 1.

while *Acetabularia* species have more cap appendages (30–90) and radially elongated coronal chambers. Our measurements on *P. peniculus* and *A. acetabulum* show that the greater number of appendages in *Acetabularia* results from a smaller spacing. Therefore, lateral interference in *Acetabularia* could be responsible for the morphogenetic contrasts between the two genera. Interestingly, intermediate morphologies are seen in species with intermediate numbers of appendages, such as *Acetabularia caliculus* (30), suggesting a morphological continuum between *Polyphysa* and *Acetabularia*. However, this trend is not as clear in other *Acetabularia* species with similar intermediate number of appendages (e.g. *Acetabularia farlowii* and *Acetabularia dentata*). Further measurements of spacing in a number of species is required to determine whether morphology varies continuously with that variable.

The second piece of evidence for the effect of lateral interference on morphology comes from *A. acetabulum* itself. Even though *A. acetabulum* has the smallest spacing and thus the highest degree of lateral interference, its coronal chambers are initially similar to the coronal chamber of *P. peniculus* (figure 4*g*). That is, the corona protuberances occur first in a whorled pattern (Valet 1968) and the coronal chambers lack radial projections. Therefore, the major differences in morphology arise after extensive growth of the laterally constrained coronal chamber has forced two radial projections along the upper and lower sides of the gametophore and stretched the corona protuberances along a radial line (figure 4*h*; Berger & Kaever 1992, p. 127).

If the simple mechanical effect of lateral interference is indeed important, a major part of the taxonomic distinction between the genera *Polyphysa* and *Acetabularia* is determined by a single parameter: the spacing between appendages in the reproductive whorl.

(ii) Batophora oerstedi

The morphology of *Batophora* differs substantially from that of *Acetabularia* and *Polyphysa*. First, the hairs are not shed. Consequently, the stalk of *Batophora* displays almost all the whorls produced during the vegetative phase of the life cycle rather than just the most recent ones. Second, the gametophores are not formed in specialized whorls such as the cap of *Acetabularia* and *Polyphysa*. Instead, they arise during a second 'differentiation wave'

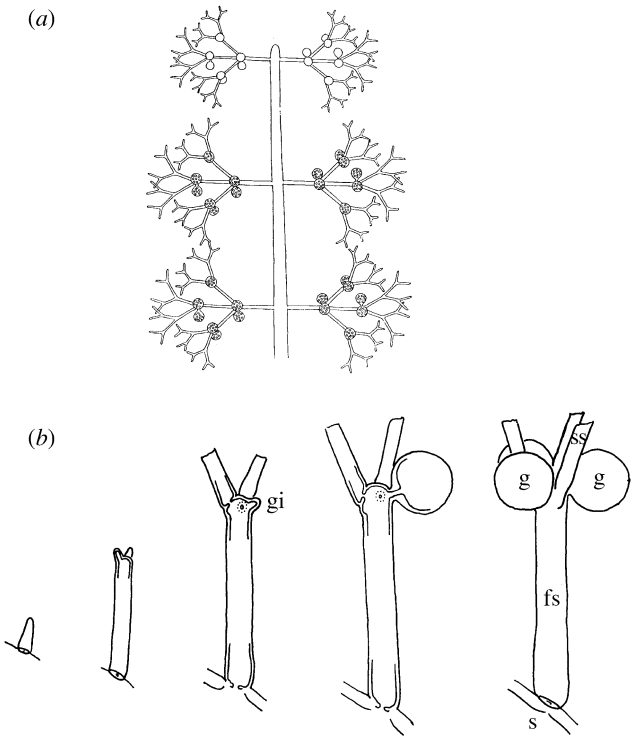

Figure 6. Morphogenesis of the reproductive whorl of *Batophora oerstedi*. (*a*) Fully developed reproductive whorl (from Berger & Kaever (1992), with permission). (*b*) Morphogenetic sequence. For abbreviations, see table 1.

on what appeared first to be vegetative whorls (figure 6). The morphogenetic stages in *Batophora* are thus the same as those described for the cap of *Acetabularia* with the important distinction that the morphology of the first five stages resembles that of the vegetative whorl. Gametophore initiation (stage 6) lags several weeks behind the actual differentiation of the thallus, during which the vegetative whorls are produced (Puiseux-Dao 1962). Usually, segments of first-, second- and third-order differentiate one to three spherical gametophores in their subapical region. The morphology of the reproductive whorl of *Batophora* is suggestive of the origin of the more specialized reproductive whorls seen in *Acetabularia* and *Polyphysa*. This question is addressed in § 5.

(iii) Neomeris stipitata

The account given here is based on Church's description of the development of *Neomeris stipitata* (Church 1895). (Church considered his specimens to be representatives of the species *N. dumetosa*, which now appears to be an incorrect identification; see Egerod 1952.) He divided the differentiation of the thallus into five developmental phases. The first four phases are morphological variations of the vegetative whorl. They will not be discussed here save to say that, as in *Batophora*, the vegetative whorls remain attached to the stalk and ultimately form a dense cortex around it. The last developmental phase leads to the elaboration of reproductive whorls. Again, the five initial morphogenetic stages are morphologically identical to those of the vegetative structure (figure 7). The gametophores are differentiated last (stage 6). They are spherical outgrowths connected to the branching point of primary hair segments via a short pedicel and a

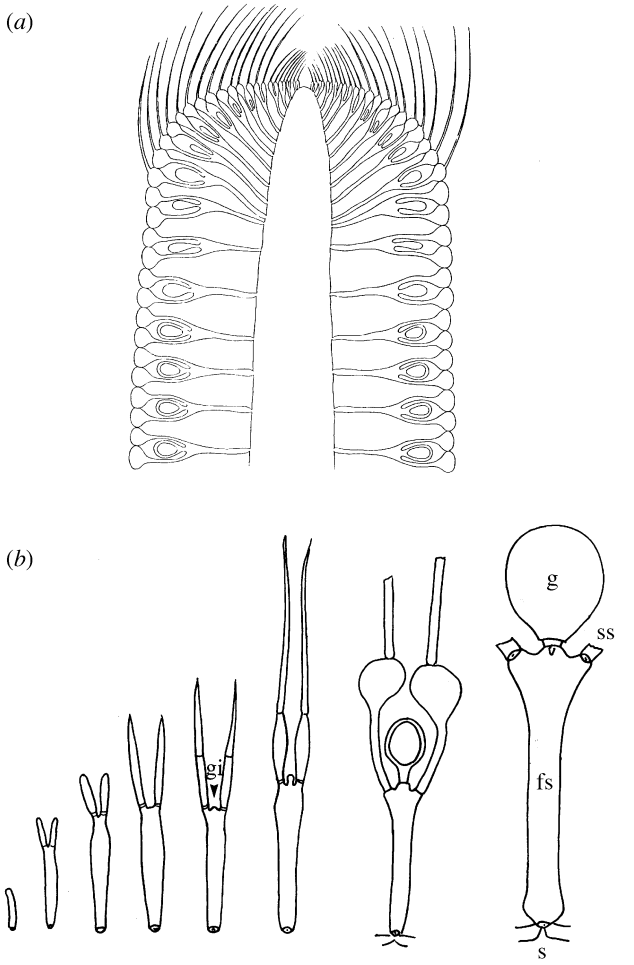

Figure 7. Morphogenesis of the reproductive whorl of *Neomeris stipitata*. (*a*) Fully developed reproductive whorl (from Berger & Kaever (1992), with permission). (*b*) Morphogenetic sequence (redrawn from Church (1895), with permission). For abbreviations, see table 1.

perforated septum. The lag between the two differentiation processes is much reduced here (Church 1895). Svedelius (1923) has observed that each gametophore is initiated in the subapical region (i.e. at the level where the second-order segments connect) and reaches its terminal position only later. The reproductive whorl of *Neomeris* is also an apparent specialization of a *Batophora*-like whorl, though quite distinct in nature from the specialization seen in *Acetabularia* and *Polyphysa*.

(iv) Halicoryne spicata

The morphology of *Halicoryne* has been described by Cramer (1895), Solms-Laubach (1895) and Okamura (1907–1909), while Valet (1968) studied its morphogenesis. The information presented in this section is drawn mostly from the latter work. After a juvenile phase where only vegetative structures are made, *Halicoryne* produces vegetative and reproductive whorls alternately. There are no major structural differences between the vegetative whorl of *Halicoryne* and that of other dasycladalean genera. However, the morphogenesis of the reproductive whorl does not follow the sequence previously described (figure 8). The young reproductive whorl contains seven to ten more or less pointed appendages

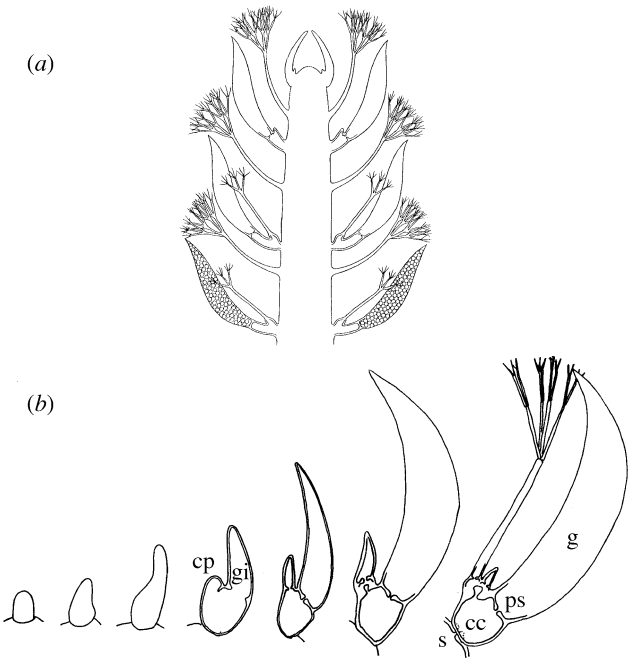

Figure 8. Morphogenesis of the reproductive whorl of *Halicoryne spicata*. (*a*) Fully developed reproductive whorl (from Berger & Kaever (1992), with permission). (*b*) Morphogenetic sequence (redrawn from Valet (1968), with permission). The last two drawings illustrate coronal chambers with one and two corona protuberances. For abbreviations, see table 1.

(stage 4). As they elongate, the basal segment (coronal chamber) first forms a gametophore. Subsequently, one or two hair initials branch off to constitute the corona superior. The hair initials and the gametophore are then partially isolated from the coronal chamber by the formation of perforated septa. In terms of pattern formation, the morphogenetic sequence previously described cannot be extended to *Halicoryne* since in this case initiation of the gametophore occurs before differentiation of the corona superior. Additional observations are needed to characterize this unusual morphogenesis and to relate it to the morphogenesis of other dasycladalean algae.

(c) *Additional observations on whorl morphogenesis*

We complete our description of morphogenesis in *Acetabularia* with an indication of the variability of the different features of whorl morphogenesis. Qualitative and quantitative variations are reported here. A number of closely regulated features are then discussed.

(i) *Variation in morphogenesis*

Most qualitative variations are considered to be teratological morphologies and have been reported as such by many authors (see references below). These observations fall into two classes: growth redirection, and organ abortion or reversion. As mentioned earlier, the appendages of the vegetative and reproductive whorls have a determinate growth in that they branch a fixed number of times and then cease growing. Several teratological morphologies reported in the literature (Solms-Laubach 1895; Valet 1968; Bonotto 1971; Menzel 1994) show a redirection of growth from the main stalk to one or several lateral appendages, thus removing their

PHILOSOPHICAL TRANSACTIONS OF THE ROYAL SOCIETY B BIOLOGICAL SCIENCES

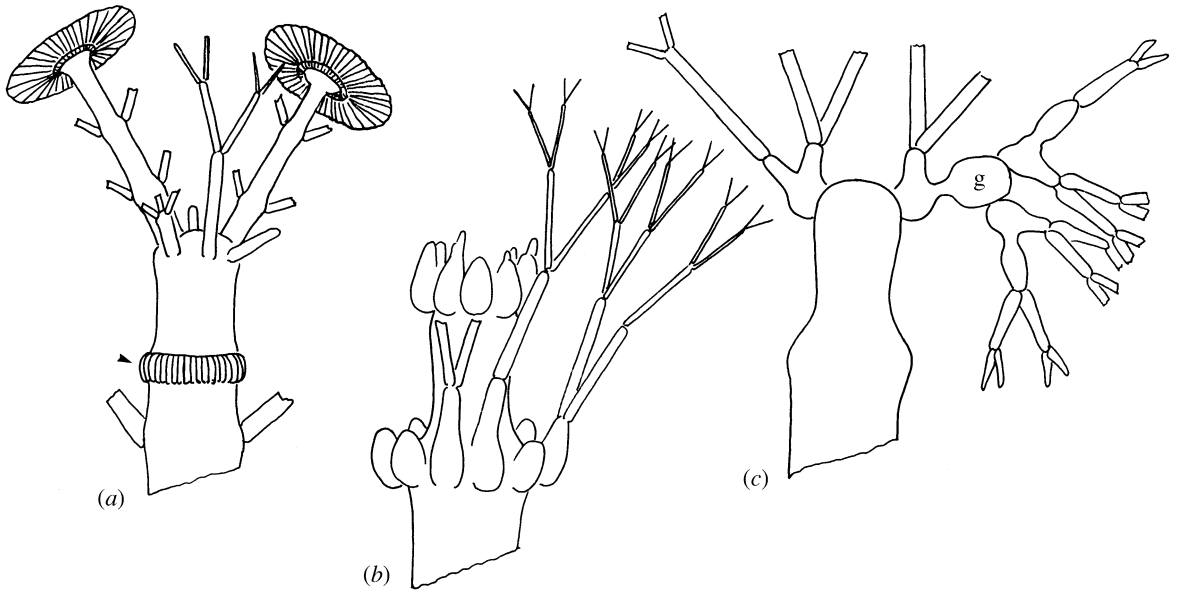

Figure 9. Variation in whorl morphogenesis. (*a*) Redirection of apical growth in *A. acetabulum*. Two hairs have each produced two vegetative whorls and a cap. Note the aborted cap below (arrow). (*b*) Two successively aborted caps in *Polyphysa peniculus*. (*c*) Hair growing on an aborted gametophore (left) and cap growing on a gametophore (right) in *Polyphysa peniculus*. For abbreviations, see table 1.

determinacy (figure 9; Dumais 1996). The newly defined growth axes usually form a series of vegetative whorls before producing a terminal cap. The second class of qualitative variation, organ abortion or reversion, is most frequent in the reproductive whorl. This can probably be explained by the fact that the morphogenesis of the reproductive whorl is more sensitive to changes in growth conditions than that of the vegetative whorl (Goodwin *et al*. 1983). Reversion from reproductive to vegetative morphogenesis is found in *Polyphysa*, *Acetabularia* and other genera (figure 9; Dumais 1996). Clearly, the mechanisms responsible for vegetative and reproductive morphogenesis are compatible, since young reproductive organs are readily transformed into vegetative organs. Other aberrant morphologies have been reported such as branching of the main axis, variation in the number and location of the cysts, and variation in the size and shape of the rhizoid, the stalk and the lateral appendages (Valet 1968; Bonotto 1969; Bonotto & Puiseux-Dao 1970; Nishimura & Mandoli 1992*b*; Mandoli 1996). Cell lines with similar abnormal phenotypes have been established (Mandoli 1996), indicating that some of them are genetically based.

Quantitative variations are seen during the maturation of the cell and when the culture conditions are changed. This suggests that, to a large extent, they correspond to variations in the physiological state of the cell. Good examples are the increase in whorl complexity (degree of branching) during the vegetative phase (Nishimura & Mandoli 1992*a*) and the lengthening of hair segments observed in cells grown in nitrogen-limited culture medium (Adamich *et al*. 1975; Gibor 1989).

(ii) *Constant morphogenetic features*

In *Acetabularia*, we have observed whorls with as few as three hairs and as many as 35 hairs. Such a variation gives the impression that whorl formation is poorly regulated. However, researchers have reported a positive correlation between the number of appendages in the whorl and whorl diameter (Church 1895; Egerod 1952). A quantitative analysis of this correlation came later (Harrison *et al*. 1981). The correlation indicates that the variation in the number of whorl appendages (n) results from the increase in tip diameter (d) during the vegetative phase of the life cycle. In fact, while the number of appendages increases throughout development, the average spacing ($\lambda = \pi d/n$) inside the whorl remains constant. This constant spacing has now been demonstrated for different species (figure 10) and for different stages of whorl development (figure 11). (Note: the whorl diameter (d) is easily obtained from wall ghosts. With *in vivo* measurements, the tip diameter is obtained, while the whorl itself is inscribed inside the perimeter of the tip (see figure 3*a*,*c*). In previous papers we used the equation $\lambda = \pi d/(\pi + n)$ to take this into account; here, for uniformity, d has been corrected when necessary so that the equation $\lambda = \pi d/n$ applies throughout.)

The uniform spacing between adjacent appendages in a whorl is conveyed quite clearly from micrographs (figures 3*a*,*c* and 4*d*). A quantitative assessment of spacing variability in single whorls is given by the coefficient of variation V for spacing (V, standard deviation/mean (Zar 1984)). A V of 100% is typical of a random pattern, while lower values are indicative of spatial order; a value of zero represents a perfectly spaced pattern. Measurements made in our laboratory have shown that in-whorl spacing is very orderly. The average V is 19% for stage 3 (wall lysis) and 14% for the stage 3–stage 4 transition. In both cases, the average is based on measurements of 14 hair whorls. The whorls of figure 3*a*,*c* are more orderly than average, with V-values of 12.4 and 8.7%, respectively. Similar measurements are not available for the

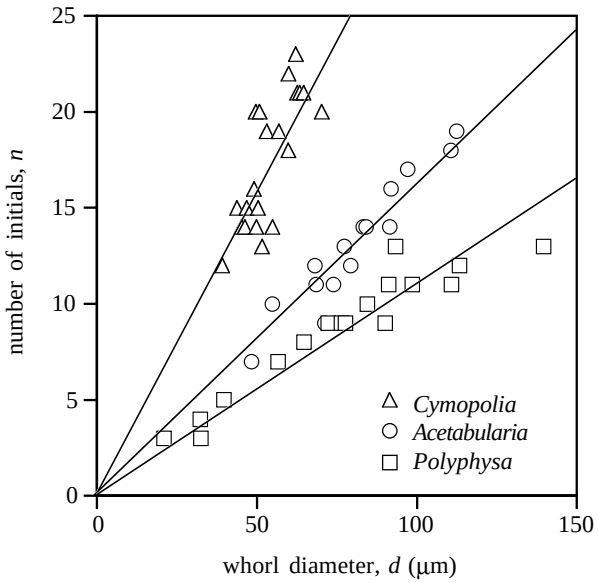

Figure 10. Number of initials (n) versus whorl diameter (d) measured at early stage 4. The linear relationship for each species is indicative of a constant spacing. The slopes (approximately π/λ) are inversely proportional to the spacing (λ). *Cymopolia van bosseae* (reproductive whorl), $\lambda \approx 11.2\,\mu m$; *A. acetabulum* (vegetative whorl) (from Harrison *et al.* (1981), with permission), $\lambda \approx 19.6\,\mu m$; *Polyphysa peniculus* (vegetative whorl), $\lambda \approx 34.9\,\mu m$.

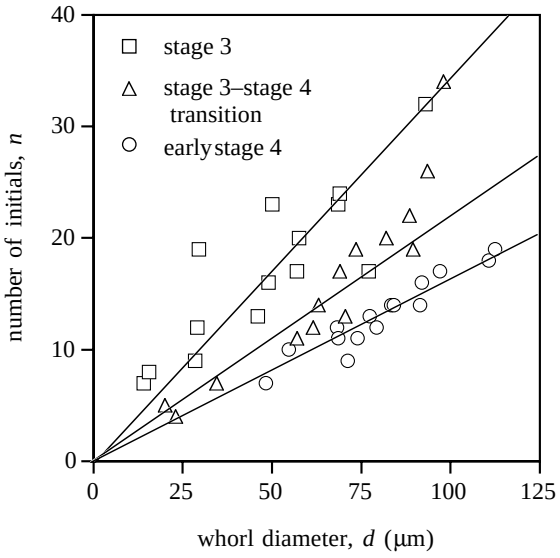

Figure 11. Number of initials (n) versus whorl diameter (d) at three stages of whorl development in *A. acetabulum*. The spacing is constant for a given developmental stage but it increases rapidly from stage 3 to stage 4 (the average λ is 8.8, 14.0 and 19.6 μm, respectively).

cap, but figure 4*d* shows that the lysis pattern is at least as orderly.

In addition to the constant spacing, whorl formation shows two other striking regularities. First, all the whorl elements are initiated simultaneously (note the uniformity in the degree of lysis in figures 3*a* and 4*d*). This contrasts with the ensuing growth of the whorl, where the degree of development can differ among appendages of a single whorl. The degree of development is sometimes randomly distributed, but in many cases it varies continuously around the whorl (see figure 3*c*; note that the gradation in size is not an artefact). Similar graded distributions are observed for the number of secondary segments in the vegetative whorl (see Berger & Kaever 1992, p. 200), as well as in cap development. Secondly, the lysis sites are confined to a narrow region around the tip (figures 3*a* and 4*d*). Staggered lysis pits are rarely seen, even if fully grown appendages sometimes appear shifted.

The simultaneous appearance of the lysis pits, their confinement to a narrow region, and their uniform spacing suggest that the dasycladalean whorl is an 'entity' (for a discussion of pattern as entity, see Harrison 1993). All appendages constituting a whorl arise together as one coordinated unit, a single pattern of repeated parts. It is only in later development that appendages may display individuality in, for example, their rate of development. This suggests that the whorl is established by the interaction of chemical and/or physical factors to provide a pattern of repeated parts, probably of wave character with repeat distance as wavelength.

A complete mechanistic explanation of whorl formation should account for the six morphogenetic stages of § 2(a) and the coordinate initiation of the whorl pattern. To date, the most complete models are limited to the first four stages of morphogenesis. However, it is significant that all the models proposed are characterized by an intrinsic wavelength that explains the constant spacing and the coordinate initiation of the whorl (see § 3).

3. MORPHOGENETIC MODELS

The morphogenetic staging of § 2 fulfils the first step of the pattern formation viewpoint. We now turn to the possible pattern-forming mechanisms. Three models have been put forward to explain whorl formation in *Acetabularia*. In a series of papers (see references below) they were shown to be sufficient to account for the most important stages of whorl formation. However, these models are biologically quite diverse. They rely on different kinds of mechanism (mechanical, chemical and mechano-chemical) and attribute organization of the whorl pattern to different cellular compartments (cell wall, cell membrane and cytoplasm). Though this diversity is disconcerting, it also provides ground for experiments devised to discriminate between the models. Two features of whorl formation have been especially fruitful for gaining insights on the patterning mechanism. They are the regulation of spacing and the role of Ca^{2+} ions. We have summarized in table 2 the major differences between the three models. It is the basis of the different tests described in § 4.

(a) *Martynov's model*

Martynov (1973, 1975) proposed that mechanical buckling of the cell wall is responsible for whorl formation. To buckle, the cell wall must be under compression. For unicellular organisms with turgor pressure such as the Dasycladales, local compression is expected for some mechanically unstable tip geometries. Conditions for instability can be derived if the geometry is simple. This led Martynov to approximate the tip as an ellipsoid. This approximation is quite good for a tip initiating a

PHILOSOPHICAL TRANSACTIONS OF THE ROYAL SOCIETY B BIOLOGICAL SCIENCES

Table 2. *Summary of the three morphogenetic models*

(The plus and minus signs mean that increase in the variable named leads to increase or decrease, respectively, in λ.)

model	type of mechanism	nature of prepattern	location of prepattern	role of Ca^{2+} ions	variables affecting λ
Martynov	mechanical	strain	cell wall	second messenger	tip radius (+) wall thickness (+)
Harrison	chemical	X and Y morphogens	plasmalemma	morphogen precursor	[A] and [B] (−) rate constants (−) X and Y diffusion coefficient (+)
Goodwin and Trainor	mechanochemical	Ca^{2+} and strain	cytosol	morphogen	elastic moduli (+) Ca^{2+} diffusion coefficient (+) $[Ca^{2+}]$ in cytosol (−)

cap but a torispherical approximation is more accurate for the vegetative tip (figure 12). The instability condition for an ellipsoidal tip geometry is $a > \sqrt{2}\cdot b$, where a and b are the major and minor semi-axes (figure 12; Timoshenko & Woinowsky-Krieger 1959). Martynov argued that the increase in tip diameter ($2\cdot a$) associated with the shift from apical growth (stage 1) to subapical growth (stage 2) leads to a mechanically unstable tip. As the diameter increases, circumferential compression develops around the tip in the region of greatest curvature. Beyond a threshold diameter, the compression is such that a series of folds form on the previously smooth tip. This corresponds approximately to figure 3*a*,*b* and figure 4*a*–*c*.

The spacing (λ) between these folds is given by the following three approximations (Martynov 1975):

$$\lambda \approx \pi(a\delta)^{1/2} \qquad (a/\delta \approx 10,\ n \approx 6,\ \text{small hair whorl}), \quad (1a)$$

$$\lambda \approx 0.54\pi(a\delta)^{1/2} \qquad (a/\delta > 10,\ n > 6,\ \text{larger hair whorl}), \quad (1b)$$

$$\lambda \approx 1.29\pi\delta \qquad (a/\delta \approx 50,\ n \approx 80,\ \text{cap}). \quad (1c)$$

The spacing depends, at least for the hair whorl, on the tip size (a) and, more importantly, on the thickness of the wall (δ). The assumption here is that δ is a measure of wall bending stiffness (i.e. a thicker wall is stiffer). The initial amplitude (e) of the folds is given by

$$e \geqslant \delta \qquad (a/\delta \approx 10,\ n \approx 6,\ \text{small hair whorl}), \quad (2a)$$

$$e \approx \delta/3 \qquad (a/\delta > 10,\ n > 6,\ \text{larger hair whorl}), \quad (2b)$$

$$e \approx \delta/40 \qquad (a/\delta \approx 50,\ n \approx 80,\ \text{cap}). \quad (2c)$$

Given that the wall thickness (δ) is about 5 µm, the amplitude of these folds would be small compared with the size of the tip itself (20 µm $\leqslant d \leqslant$ 90 µm for the lysis stage of the vegetative whorl). Therefore, even if at the first sign of the whorl pattern (i.e. the lysis pattern) the tip does not show conspicuous folding, a pre-pattern of strain could already be present. The strain pre-pattern would form a template for the local wall lysis and the subsequent growth of the appendages. The strain could be transduced via stretch-activated ion channels (Garrill *et al*. 1993), leading to H^+ extrusion, hydrolysis of the cell wall and wall relaxation. Additionally, Ca^{2+} ions could act as second messengers in the transduction of the strain pattern into localized growth (Trewavas & Knight 1994; Knight *et al*. 1995). Note that Martynov's model depends on an initial pattern-forming event for the transition from stage 1 to stage 2 for which the author has provided no explanation.

(b) *Harrison's model*

Harrison's model is based on Turing's reaction–diffusion theory. Turing (1952) showed that specific interactions between two molecules (X and Y morphogens) can lead to a stable pattern of high and low concentration of these molecules. Maynard Smith's graphical description of how reaction–diffusion mechanisms work is shown in figure 13 (Maynard Smith 1968). Most likely, one or both of these morphogen molecules would be integral membrane proteins (Harrison *et al*. 1997). One of the simplest reaction–diffusion systems is the Brusselator (Prigogine & Lefever 1968). It is composed of the following chemical reactions where A and B are immediate precursors of the X and Y morphogens:

$$\mathrm{A} \xrightarrow{a} \mathrm{B}, \quad (3a)$$

$$\mathrm{B} + \mathrm{X} \xrightarrow{b} \mathrm{Y} + D, \quad (3b)$$

$$\mathrm{Y} + 2\mathrm{X} \xrightarrow{c} 3\mathrm{X}, \quad (3c)$$

$$\mathrm{X} \xrightarrow{d} E, \quad (3d)$$

X and Y are both diffusible, with unequal diffusivities $D_Y > D_X$. The variables a, b, c and d are the rate constants of the different reactions. Harrison's model includes two such reaction–diffusion systems in series, the output X (reaction 3*c*) of the first serving as an input A (reaction 3*a*) of the second (figure 14). The first system accounts for the transition from a growth maximum at the apex to a subapical growth annulus (i.e. it is the pattern-forming event separating stage 1 and stage 2). The second system feeds on this annular region and breaks it into a whorl pattern (transition from stage 2 to stage 3). The two systems are required for theoretical and empirical reasons. A single reaction–diffusion system operating on a hemispherical tip does not lead to a whorl pattern. Rather, higher modes, beyond the annular pattern, would most likely produce a random distribution of the morphogen peaks (Harrison *et al*. 1988). To generate whorls, irrespective of tip size, the two-step process described above is required.

PHILOSOPHICAL TRANSACTIONS OF THE ROYAL SOCIETY B BIOLOGICAL SCIENCES

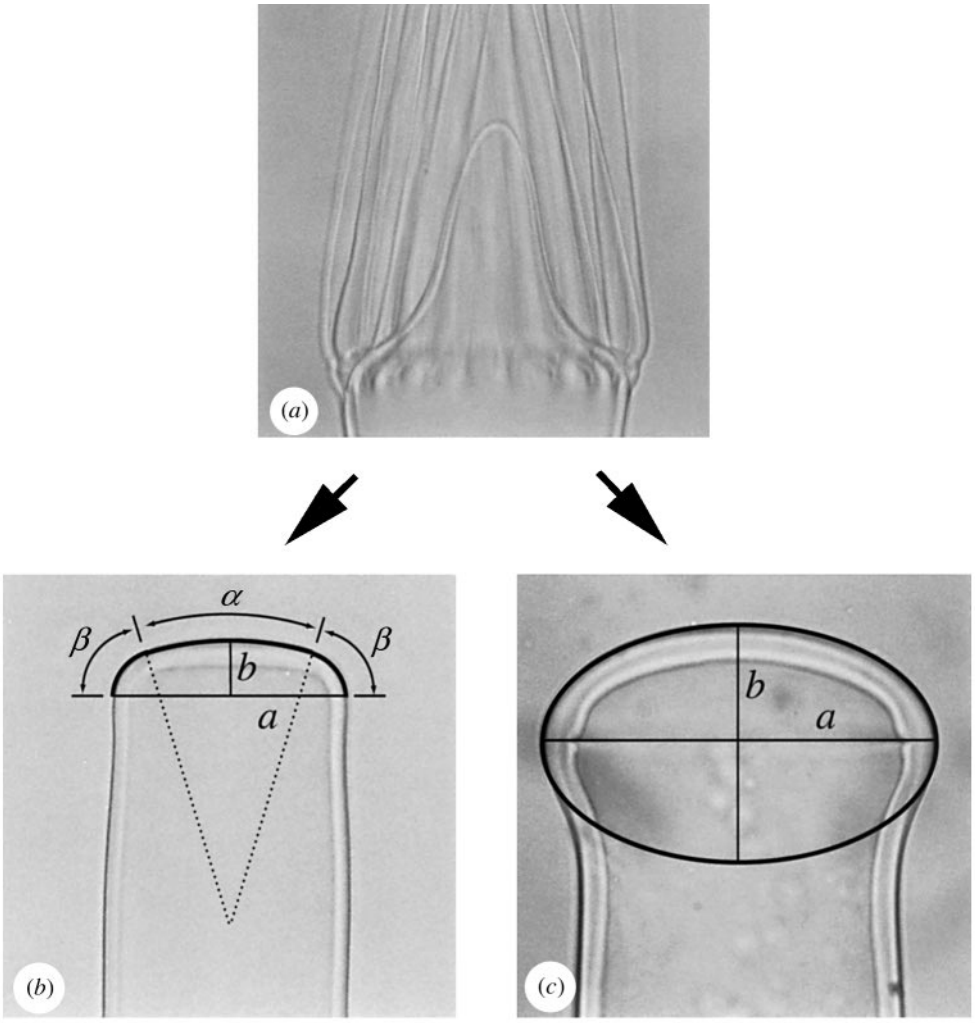

Figure 12. Schematic description of Martynov's model. (*a*) The growing tip is usually pointed. (*b*, *c*) When a whorl is initiated, growth of the subapical region causes the tip to flatten. At this stage, the vegetative tip (*b*) is best approximated by a torispherical geometry, that is, by a spherical cap (α) surrounded by a toroidal segment (β). At a similar stage, the reproductive tip (*c*) has an ellipsoidal geometry. These tip shapes are mechanically unstable if there is some internal turgor pressure. A whorl pattern would then be expected to develop in the toroidal region for the vegetative tip or in the equatorial region for the reproductive tip. This is in fact what is observed.

§4 provides most of the empirical evidence for the two systems.

Assuming that the second reaction–diffusion system is of Brusselator type, the spacing (λ) is given by the following equation (Harrison & Hillier 1985):

$$\lambda = 2\pi\left(\frac{D_X D_Y}{(a^2bc/d^2)([A]^2[B])}\right)^{1/4}. \qquad (4)$$

All two-morphogen reaction–diffusion mechanisms give dependences of λ on inverse powers of input concentration ([A] and [B] in equation (4)). The effect of these parameters on λ has been tested (see §4). The evidence suggests a role for Ca^{2+} in binding and thus activating a membrane protein (X morphogen). The transduction of the morphogen pre-pattern into growth could be achieved in several ways. For instance, Harrison *et al.* (1981, 1988) envisaged the Xs of both systems as catalysts for cell membrane extension (e.g. docking proteins for Golgi vesicles), which could account for the localized secretion of lytic enzyme and incorporation of new wall material, both being required for growth. An overview of the application of Brusselator-type mechanisms to morphogenesis in desmids, *Acetabularia*, and diatoms was given by Lacalli (1981).

(c) *Goodwin and Trainor's model*

Goodwin & Trainor (1985) put forward a model for whorl formation in *Acetabularia* involving an interaction between the cytoskeleton and cytosolic Ca^{2+}. This interaction affects the viscoelastic state of the cytoplasm and can therefore be used to generate a field of stresses acting mechanically on the cell membrane and the cell wall. The mechanochemical interaction is diagrammed in figure 15 (see also Oster & Odell 1984). First, the mechanical state of the cytoplasm influences the free cytosolic [Ca^{2+}]. If the system is under tension, [Ca^{2+}] increases; if the system is compressed, [Ca^{2+}] decreases. Second, [Ca^{2+}] influences the mechanical state of the system. An increase in cytosolic [Ca^{2+}] induces a solation of the cytoplasm (lower viscosity), whereas a decrease of [Ca^{2+}] induces gelation (higher viscosity). The calcium concentration is also assumed to influence the elastic modulus of the cytoplasm in a complex fashion. Contrary to the previous two

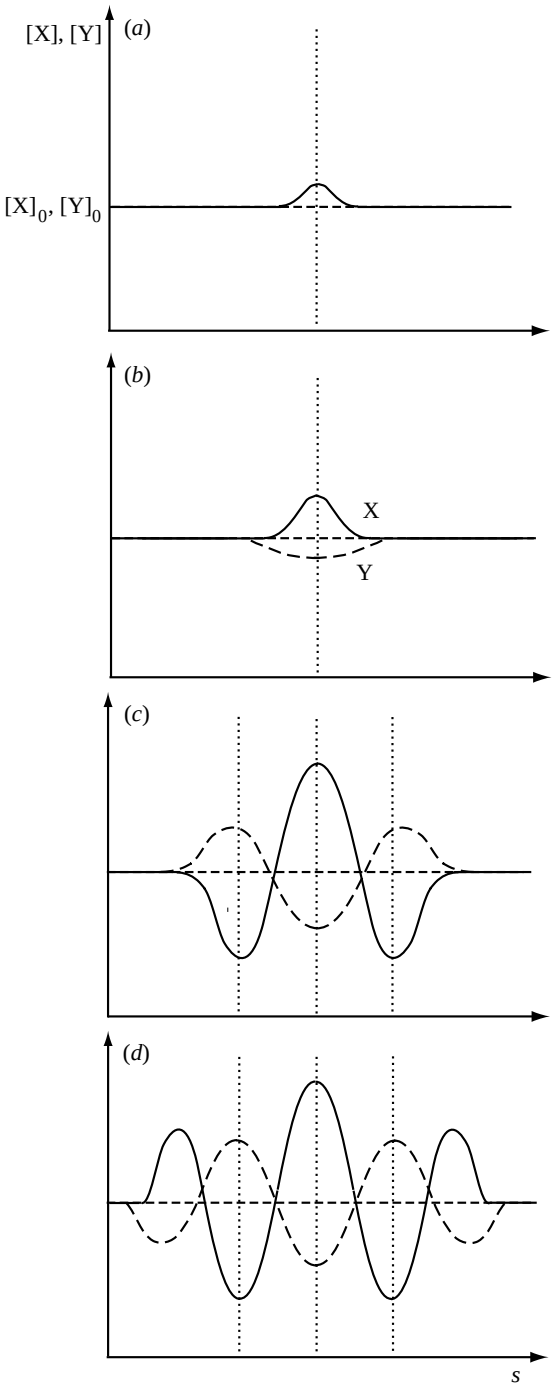

Figure 13. Schematic description of the dynamics of a Brusselator mechanism. Each graph represents the concentration of the two morphogens (X, Y) along one spatial dimension (S). (*a*) A small perturbation from the homogeneous steady state ($[X]_0$, $[Y]_0$) of one of the morphogens (here X) leads to (*b*) an increase in X (X catalyses itself) and a depletion of Y (X uses up Y for its own catalysis). Since Y diffuses faster than X, the trough in Y distribution will enlarge faster than the peak in X distribution. In the periphery, where $[X] = [X]_0$ but $[Y] < [Y]_0$, the production of X is decreased (Y is needed for the steady production of X). (*c*) The decrease of [X] below $[X]_0$ enables [Y] to rise above $[Y]_0$. At the same time the initial X peak and Y trough approach new steady-state values. (*d*) Further propagation in the system will create a series of peaks and troughs in the [X] and [Y] distributions. Each peak could drive the differentiation of one whorl initial. Modified from Maynard Smith (1968).

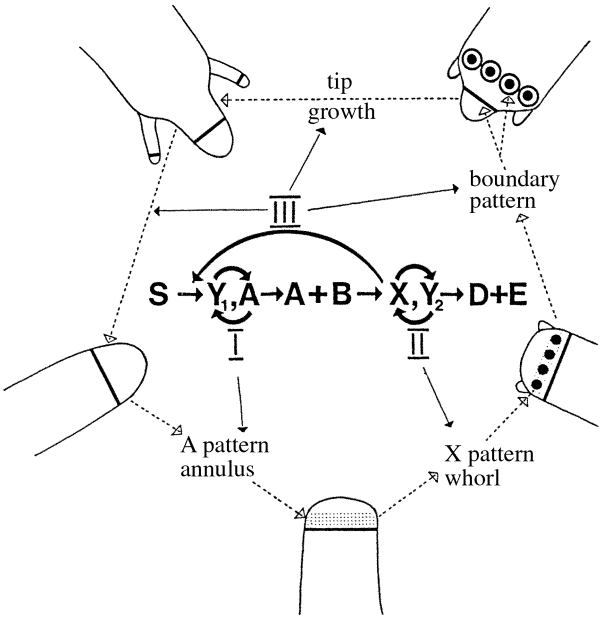

Figure 14. The two-stage model for whorl morphogenesis in *Acetabularia*. The two stages are the feedback loops I and II. They represent two Brusselators in sequence, the X morphogen of loop I being designated A because it is the A reactant for loop II. A third feedback loop is required to account for the sequential production of whorls. It controls the movement of the tip's boundary as it grows. S is initial reactant or reactants. From Harrison (1992), with permission of the University of Chicago Press.

models, Ca^{2+} ions are involved directly as morphogens in this model.

The equation for the spacing has not been written explicitly, but computations have shown the effect of a series of parameters on λ (Brière 1994):

$$\lambda \text{ increases with } ([Ca^{2+}]_t^{-1}, D_\chi, \mu, \nu), \quad (5)$$

where $[Ca^{2+}]_t$ is the total intracellular Ca^{2+} concentration, D_χ is the diffusion coefficient of Ca^{2+}, and μ and ν are the constants of elasticity. All these parameters have a physical meaning, but most of them are not readily accessible to measurement. Goodwin & Trainor (1985) proposed that the strain prepattern could be transduced into growth by stretch-activated ion channels. This could lead to a secretion of H^+ ions, inducing local lysis of the cell wall.

4. TESTING THE MODELS

(a) *Effects of temperature on spacing*

With their reaction–diffusion model, Harrison *et al.* (1981) have considered the possibility that chemical reaction rates, together with transport (diffusivity of at least two substances), control whorl formation. Reaction rates are among the most temperature sensitive of all physical and chemical properties. Diffusivities are also temperature sensitive, but to a lesser degree. In general, both increase with temperature. Since the parameters that increase most rapidly with temperature appear in the denominator of the expression for spacing (equation (4)), λ is expected to decrease as temperature (T) rises. This

PHILOSOPHICAL TRANSACTIONS OF THE ROYAL SOCIETY B BIOLOGICAL SCIENCES

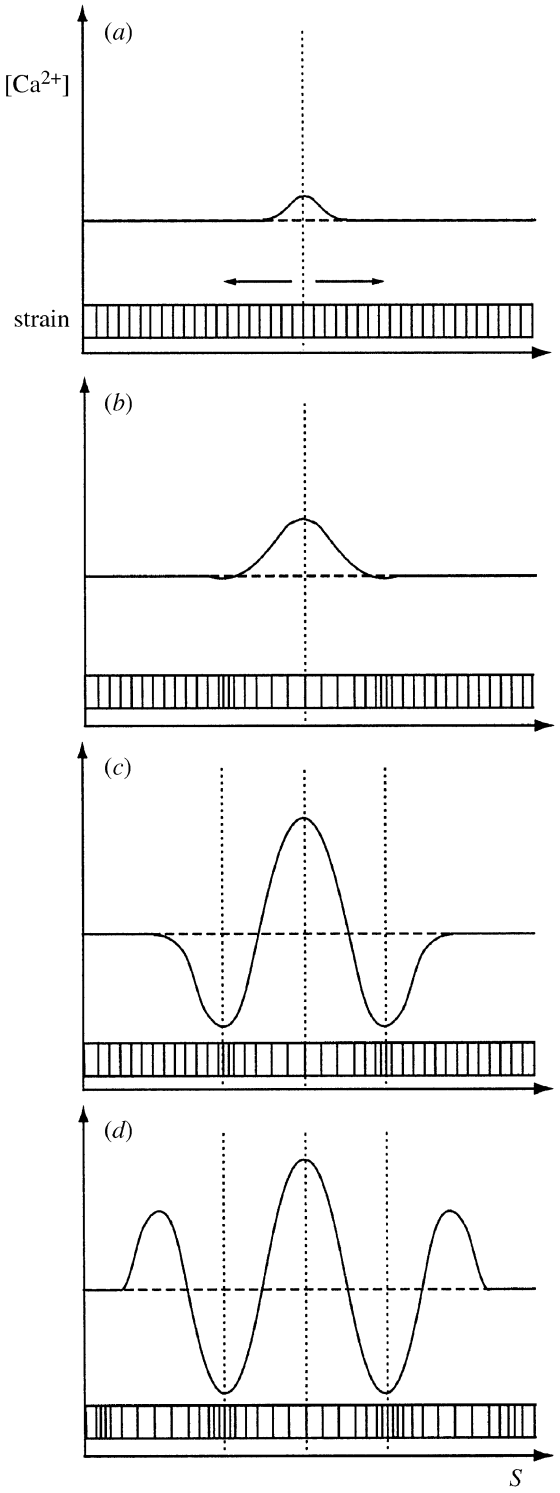

Figure 15. Schematic description of the dynamics of Goodwin and Trainor's model. Each graph gives the free $[Ca^{2+}]$ and the distribution of strain along one spatial dimension (S). (a) The gradients of free Ca^{2+} brought about by a small perturbation from the homogeneous steady-state concentration induce opposite forces on the two sides of the perturbation (arrows). (b) As a result, the central cytoplasmic region will be stretched, while the periphery will be compressed. Because mechanical signals are fast and diffusion is slow, regions will develop where the cytoplasm is compressed while the $[Ca^{2+}]$ is still at the steady-state level. (c) Since the mechanically compressed cytoplasm offers more binding sites for free Ca^{2+}, the free cytosolic $[Ca^{2+}]$ will drop. This will affect the mechanical state of the cytoplasm in that region and increase the local compression up to a certain point. (d) The compression will stretch the cytoplasm in the periphery, reducing the number of binding sites available. Therefore the $[Ca^{2+}]$ will rise and propagate the initial perturbation across the system. In this model, the local variations in strain and free $[Ca^{2+}]$ lead to the formation of whorl initials.

was found experimentally in *A. acetabulum* vegetative whorls (figure 16). The form of the variation even seemed to be best linearized by plotting the logarithm of λ against $1/\mathcal{T}$, the expected (Arrhenius) linearization for reaction rates (including diffusion) (Harrison *et al*. 1981). It is unlikely that the rapid decrease of λ with increasing $\mathcal{T}$ results from a direct effect of temperature on material properties since physical variables such as the modulus of elasticity usually require much larger variations of temperature to change significantly. On the other hand, it is not excluded that temperature could act indirectly by changing the rate of some chemical reactions involved in controlling the material properties of the wall. Combinations of mechanics with chemistry, as in the Goodwin—Trainor model, could be directly sensitive to temperature, so the temperature dependence is not strong evidence against this type of model.

(b) *Effects of Ca^{2+} concentration on spacing*

Molecules with putative morphogenetic roles are of course legion. One that has been involved in all three mechanisms presented above, as in many other biological processes, is calcium ion. It is known (Harrison & Hillier 1985) that the spacing λ decreases as the calcium concentration in the culture medium ($[Ca^{2+}]_e$) increases, and that the variation of λ with $1/[Ca^{2+}]_e$ is linear and temperature sensitive (figure 17). These observations must be explained by the models.

Ca^{2+} binds to pectin and causes gelation (stiffening) of this polysaccharide (Tepfer & Taylor 1981). Since pectin constitutes a substantial fraction of plant walls, a $[Ca^{2+}]$ dependence for spacing is expected in Martynov's model; but the dependence would be the opposite of that observed. The observed dependence could arise in the Goodwin–Trainor model if $[Ca^{2+}]_e$ affects intracellular $[Ca^{2+}]$. However, there is evidence that the cells, which normally face an environmental free $[Ca^{2+}]$ roughly 10^4 times greater than free cytosolic $[Ca^{2+}]$, regulate their intracellular level against changes in the extracellular one (Amtmann *et al*. 1992).

For Harrison's reaction–diffusion model, the quantitatively determined form of variation of λ with $[Ca^{2+}]_e$, and of this variation with $\mathcal{T}$, has been interpreted (Harrison & Hillier 1985) in terms of binding of Ca^{2+} to an extracellular receptor site of an integral membrane protein, activating that macromolecule to become a precursor to a Turing-type morphogen. This interpretation is the only one that has been elaborated in full physicochemical detail. Recently, it has been extended to the effect of EGTA (ethylene glycol-bis(β-aminoethyl ether) N,N,N′,N′-tetraacetic acid) as an non-competitive inhibitor of the Ca^{2+} effect (Harrison *et al*. 1997). This does not rule out the Goodwin–Trainor model, which could also involve factors of chemical binding, but it challenges the advocates of that mechanism to elaborate the $[Ca^{2+}]$ effect in similar detail.

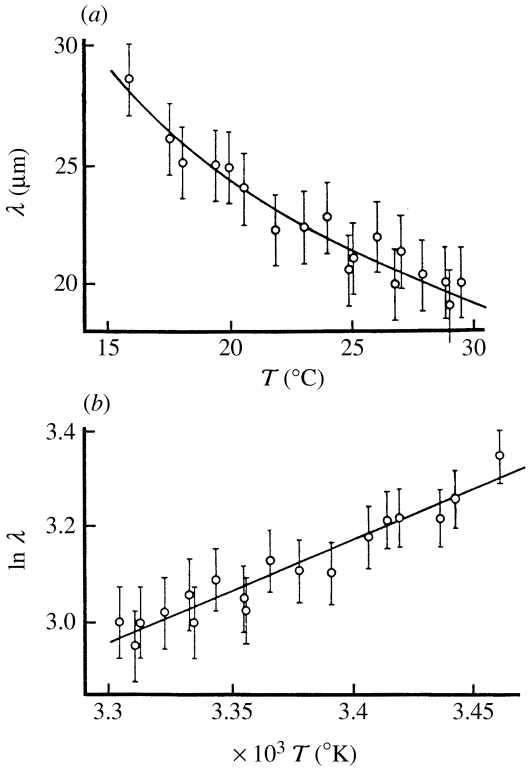

Figure 16. Temperature dependence of spacing. (*a*) Spacing (λ) versus temperature (T). (*b*) The dependence is linearized by an Arrhenius plot. In that sense, the spacing λ behaves like chemical variables, suggesting a role for variables such as reaction rate or diffusion rate in the regulation of λ. From Harrison *et al*. (1981), with permission.

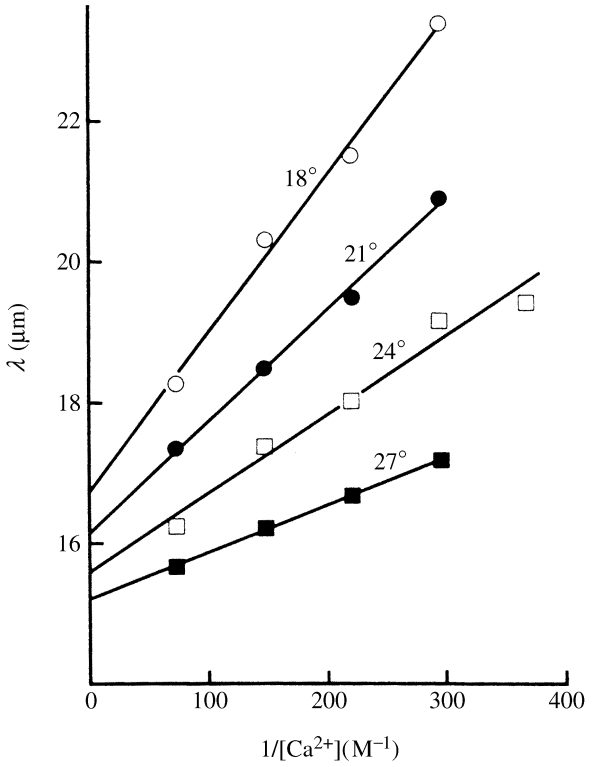

Figure 17. Effect of extracellular [Ca^{2+}] on spacing. Each point is the mean of 16 to 36 measurements. From Harrison & Hillier (1985), with permission.

(c) *Effects of wall thickness and tip geometry on spacing*

Since buckling depends on compressive stresses, evidence for such stresses is needed. Our microscope observations enabled us to test this requirement. The results are published here for the first time. Photographs such as figure 3*a*,*b* were used to assess the tip geometry (δ, a, b) of 13 vegetative whorls at stage 3. The results, based on an ellipsoidal approximation of the tip geometry, are consistent with the presence of circumferential compression in the subapical region of most cells (figure 18). Three cells lie close to but not quite beyond the threshold line for instability. These cells should lack any compressive stresses, although it is possible that a more precise approximation of the tip geometry would predict the presence of compression in these cells too.

Martynov (1975, 1976) tested the effect of structural rigidity (δ/a) on the number of initials (n) in the whorl. His experimental results are in agreement with those predicted by the theory (figure 19). Our own data for the vegetative whorl confirm to some extent his results (data not shown). However, the test performed by Martynov is not fully satisfying as a means to discriminate between the models. The major shortcoming of his approach is that all the models predict an increase in the number of initials (n) with increasing tip size ($2\pi a$). Therefore, a correlation between n and a/δ is not entirely specific to his model. The truly exclusive feature of mechanical buckling is the dependence of λ on wall thickness (δ) and tip size (a) as stated in equation (1*a–c*). We tested the validity of these equations for the vegetative whorl with the set of photographs described above. The data available do not confirm the model's predictions (figure 20); that is, we could not find a significant correlation between the observed spacing and the spacing predicted from the equations ($r = 0.341$, $P > 20\%$). For the reproductive whorl, equation (1*c*) predicts a spacing approximately four to five times larger than the wall thickness. Figure 4*e*,*f* indicates that the spacing is actually less than half the wall thickness. These results are evidence against mechanical buckling as formulated by Martynov, but objections are possible. First, the analysis is based on an ellipsoidal approximation of the tip. An approximation that conforms more closely to the tip's geometry would potentially yield better results. Second, the assumption that wall thickness (δ) is directly related to wall stiffness may not be valid. In particular, stiffness depends also on the chemical composition of the wall. A direct measurement of wall bending stiffness would address this problem. Finally, since the wall of *Acetabularia* is composed of at least two layers (Kof *et al*. 1987), it is possible that pattern formation depends only on the buckling of the inner wall layer where the lysis first appears. This would be consistent with the observation in some *Polyphysa* species that a substantial portion of the wall, called the pectic velum, is not involved in the formation of the whorl initials. The velum is instead pushed away by the whorl growing underneath (see Valet (1968), plate 14(3), or Puiseux-Dao (1972), plate 1). However, our observations of whorl initiation in *A. acetabulum* have provided no such evidence.

PHILOSOPHICAL TRANSACTIONS OF THE ROYAL SOCIETY B BIOLOGICAL SCIENCES

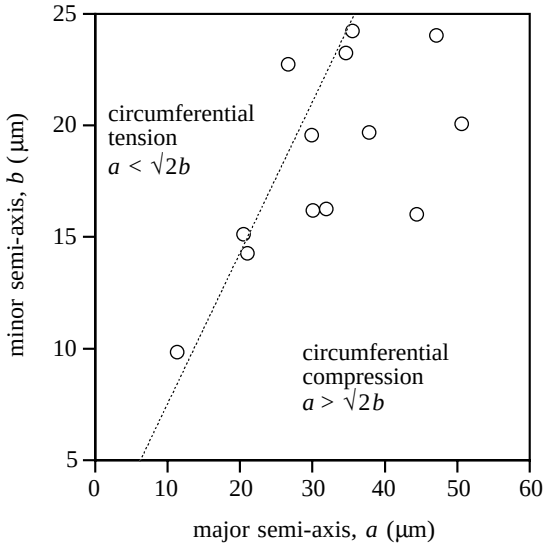

Figure 18. Evidence for compressive stresses in vegetative tips when the whorl pattern is being established (stage 3). All points to the right of the threshold line $a = \sqrt{2}{\cdot}b$ represent cells with a mechanically unstable geometry and compressive stresses are predicted. The points to the left should not have any compressive stresses if the approximation of the tip geometry as an ellipse is accurate.

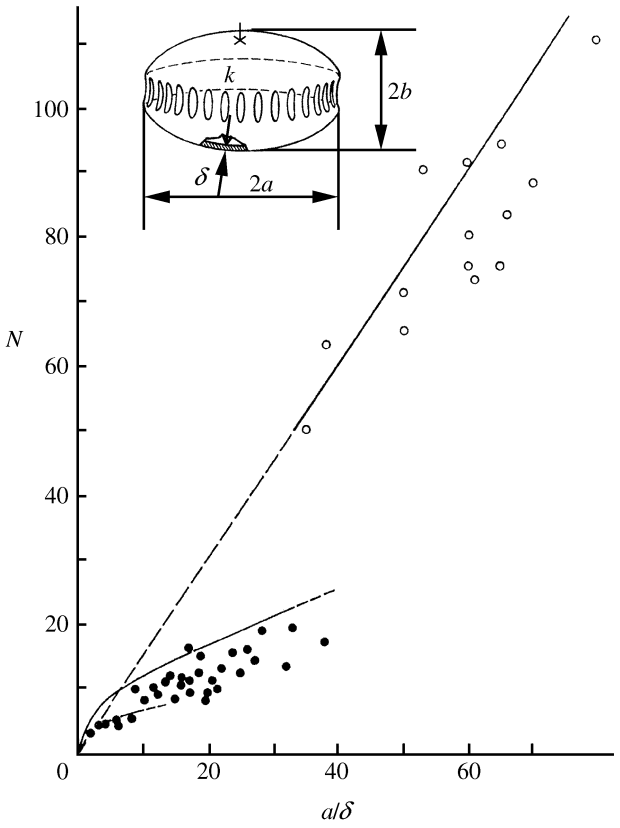

Figure 19. Dependence of the number of hair initials (N) on the inverse of structural rigidity, $(\delta/a)^{-1}$. The curves represent the relationships expected from the theory (open circles, reproductive whorls; filled circles, vegetative whorls). The insert shows the ellipsoidal approximation of the tip geometry as well as the different variables involved. Modified from Martynov (1975), with permission.

(d) *Distribution of Ca^{2+} ions*

A prepatterned distribution of a chemical substance, in advance of the appearance of any morphological pattern, is often sought to explain morphogenesis. For whorl formation on a growing tip, what molecules should constitute the pre-pattern and what geometry of pre-pattern should one expect to see? The control of λ by extracellular $[Ca^{2+}]$ and the direct or indirect involvement of Ca^{2+} ions in the mechanisms postulated by the three models indicate that this ion is a good candidate.

An essential feature of the three models presented is that the entire whorl pattern is an entity. For reaction–diffusion, that entity includes spatial distributions of morphogens X and Y in a whorl pattern, provided that their immediate precursors A and B have previously become distributed in an annular pattern. Now the spacing λ, as given by equation (4), is dependent on [A] and [B], and not upon [X] and [Y]. Therefore, if control of λ is of this type, we expect to see a pre-pattern of A or B in annular form, with no indication of the whorl pattern. Having shown in §4(b) that λ depends on $[Ca^{2+}]_e$, we would expect an annulus of Ca^{2+} to be compatible with Harrison's model. Ca^{2+} is a morphogen in Goodwin and Trainor's model (Goodwin & Trainor 1985) and should therefore form a pre-pattern prior to the initiation of the appendages. The buckling mechanism proposed by Martynov makes no explicit assumptions for the distribution of Ca^{2+} ions. In all cases, Ca^{2+} ions are potentially involved in maintaining apical growth. High $[Ca^{2+}]$ is thus expected in regions of active growth.

Earlier work using chlorotetracycline (CTC) to visualize membrane-bound Ca^{2+} (Reiss & Herth 1979) and aequorine to specifically target free cytosolic Ca^{2+} (Cotton & Vanden Driessche 1987), has demonstrated a high Ca^{2+} concentration at the growing tip of the stalk and hairs. Cotton & Vanden Driessche (1987) reported that the apical gradient of Ca^{2+} disappeared as soon as the cap is initiated. The discovery of a parallel distribution of calmodulin (Haußer *et al.* 1984; Cotton & Vanden Driessche 1987) suggests that the ion and the protein could act together in a signal transduction pathway (Vanden Driessche 1990).

Similar work was undertaken to visualize Ca^{2+} ions specifically when the whorl pre-pattern is laid down (figure 2l; Harrison *et al.* 1988; Dumais 1996). The detailed observations using CTC showed a redistribution of membrane-bound Ca^{2+} from a terminal maximum to a subapical annulus as the tip broadens to initiate a whorl (figure 2l*a*). The Ca^{2+} fluorescence shows whorl patterning only after each element of the whorl has been definitely formed morphologically. As with the vegetative whorl, the early stage of cap formation is characterized by a ring of fluorescence circling the tip. This ring, initially continuous, breaks down into a series of bright spots soon after the appearance of the cap initials (figure 2l*c*). Preliminary work using micro-injected fluo-3 (Molecular Probes, Eugene, OR, USA) to reveal free cytosolic Ca^{2+} provided similar results. A flattened tip initiating a hair whorl (stage 3) is characterized first by an annulus of fluorescence (figure 2l*b*). Similarly, in a young cap where the initials have just appeared (early stage 4), a continuous region of fluorescence circles the tip (figure 2l*d*). In

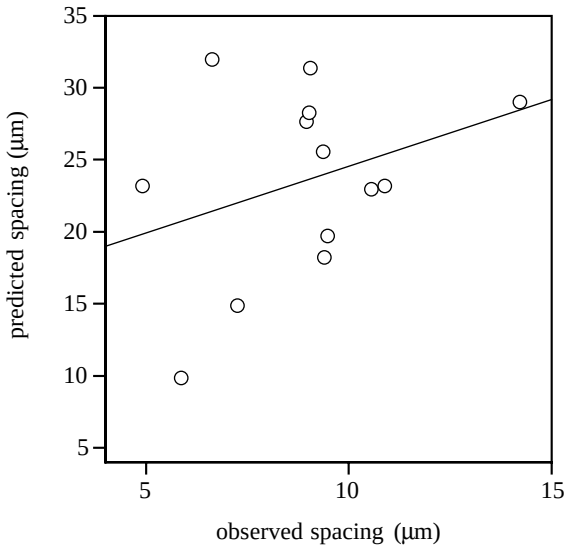

Figure 20. Test of Martynov's model. The predicted spacing, based on equations (1*a*,*b*), is plotted against the observed spacing. There is no significant correlation between the two variables ($r = 0.341$, $P > 20\%$).

both cases the fluorescence defines a region contrasting sharply with the rest of the stalk and remains an uninterrupted annulus until the whorl initials are morphologically visible. The similar Ca^{2+} dynamics between the vegetative and reproductive whorls are compatible with the similarities found in their morphogenesis (see § 2). This is nevertheless different from the earlier report of a complete disappearance of the Ca^{2+} gradient as soon as the cap is initiated (Cotton & Vanden Driessche 1987). This discrepancy remains unexplained. A detailed ratiometric study of the distribution of Ca^{2+} through morphogenetic stages 2 to 4 might prove very informative.

The results show that growth and Ca^{2+} ions are in lock-step, but there is as yet no evidence for a Ca^{2+} pre-pattern pre-figuring morphological differentiation. The absence of pre-pattern runs counter to Goodwin and Trainor's model but is compatible with the remaining models. This is in accord with the concept that Ca^{2+} initiates the pattern-forming mechanism by activating membrane-bound proteins. In this case, the whorl pattern should first be expressed by these proteins. Werz (1959, 1965) described such a protein pre-pattern but his observation was not characterized further. More recently, Menzel (1996) reported that actin marks the location of lytic sites in the morphogenetic annulus.

(e) *Conclusion*

The results presented above are most consistent with morphogenetic mechanisms based, at least partly, on chemistry (§§ 4(a) and (b)). They also strongly implicate Ca^{2+} in the mechanism but probably not as morphogen (§ 4(d)). Though this evidence does not prove the involvement of reaction–diffusion, it certainly suggests that mechanisms of this type are quite promising. On the other hand, the buckling mechanism, as formulated by Martynov (1975), appears to be unsatisfactory (§ 4(c)). The absence of an explicit expression for λ in terms of mechanical and chemical parameters precludes a quantitative assessment of this aspect of the Goodwin–Trainor model.

5. EVOLUTION OF DASYCLADALEAN MORPHOGENESIS

The dasycladalean algae have an extensive fossil record owing to their natural tendency to form calcareous skeletons. The first representatives appeared around 570 million years ago (Myr), in the Cambrian period (Herak *et al*. 1977). To date, 200 genera have been reported totalling almost 900 species (Barattolo 1991). Compared with these numbers, the 11 extant genera (38 species) represent only a small fraction of the former diversity of the group. Therefore, a clear understanding of the morphogenesis of extant genera may depend on a parallel understanding of their derivation from ancestral forms. In this section, we give a general impression of the evolutionary trends leading to the extant genera and provide mechanistic explanations for some evolutionary advances.

(a) *Major evolutionary trends*

Two trends, first described by Pia (1920), show how morphogenesis has changed during the evolution of the dasyclads. The first trend pertains to the elaboration of the thallus (figure 22). The earliest fossils attributed to the dasyclads show an irregular stalk, often branching or even anastomosing, with a dense and random arrangement of appendages (Herak *et al*. 1977). However, morphologies characterized by a cylindrical main axis became predominant early in the evolution of this group (i.e. 435–570 Myr). In the first well-defined morphological type, the lateral appendages remained randomly distributed along the central axis (aspondyl morphology). The aspondyl morphology was gradually replaced by forms bearing true whorls of unbranched appendages (euspondyl morphology). The aspondyl–euspondyl transition may have occurred between three (Pia 1923) and seven times (Kamptner 1958). The earliest instance of this transition occurred in the Ordovician (435–500 Myr) but most euspondyl lines emerged in the Carboniferous (290–360 Myr) (Kamptner 1958). During that period other morphological types (metaspondyl, mesospondyl) were present although they may not have played a dominant role in the evolutionary trend leading to the extant genera. The most derived morphological type (250 Myr to present) has an euspondyl morphology with branched appendages. All extant species fall in this latest group.

The second evolutionary trend pertains to the location of the reproductive, cyst-bearing, structures. It includes four morphological types (figure 22; Barattolo 1991), each new type shifting the reproductive structures to a more distal position. Originally, the cysts were contained inside the central cavity (endospore morphology). The earliest fossil evidence of endospore taxa dates from the Cambrian period (500–570 Myr) (Berger & Kaever 1992) but endospore taxa reappear sporadically throughout the fossil record. In the Carboniferous (290–360 Myr), a second morphological type emerged where the cysts were contained in the primary hair segments (cladospore morphology). By that time, the euspondyl morphology was already established; the cysts were thus located inside the segments of whorled appendages. In the Triassic (205–240 Myr), a third morphological type appeared with specialized cyst-bearing appendages, the gametophores.

PHILOSOPHICAL TRANSACTIONS OF THE ROYAL SOCIETY B BIOLOGICAL SCIENCES

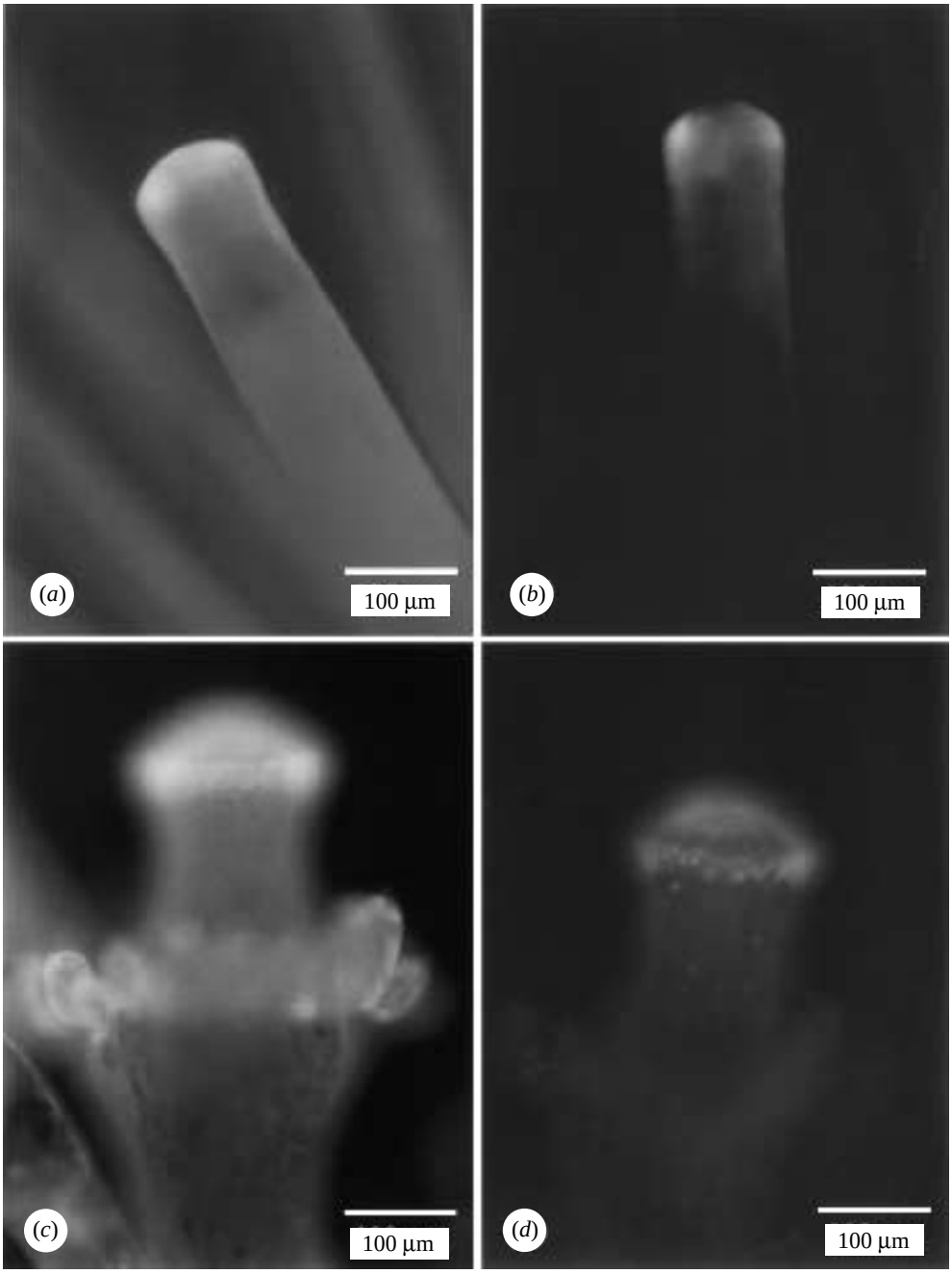

Figure 21. Distribution of membrane-bound and free cytosolic Ca^{2+} in *A. acetabulum*. (*a*) Stage 3 vegetative whorl showing an annulus of strong Ca^{2+}-CTC fluorescence. (The annulus is more readily seen during microscopic observation, here the two lateral bright spots indicate its presence.) (From Harrison *et al*. (1988), with permission). (*b*) Cell at the same stage as (*a*) but micro-injected with fluo-3. The distribution of free cytosolic Ca^{2+} is strikingly similar to that in (*a*). (*c*) Stage 4 reproductive whorl stained with CTC. The fluorescence is greater in the young cap appendages. (*d*) Stage 4 reproductive whorl stained with fluo-3. The zone of morphogenesis contrasts sharply with the remainder of the stalk. The brighter spots result from an uneven distribution of chloroplasts. (Photographs *b*, *c* and *d* from Dumais (1996).)

This is the choristospore morphology to which the present families Dasycladaceae and Acetabulariaceae conform. Valet (1968) proposed that the common ancestor of the two families was similar to *Batophora* although the fossil record would rather suggest an ancestor with features similar to the extant genera *Cymopolia* and *Dasycladus* (figure 22; Berger & Kaever 1992). The divergence of the two families dates back to approximately 205 Myr. The Dasycladaceae line includes forms with elongated primary segments and spherical to subspherical gametophores. In several genera, segments of second order are enlarged. In the Acetabulariaceae, the number of reproductive structures is usually reduced to one or a few terminal whorls. The primary segments of these whorls are reduced in length, the gametophores are elongated, and higher-order segments (i.e. the hairs growing from the corona superior) remain unchanged. Because of this extensive remodelling, the reproductive whorl in the Acetabulariaceae is morphologically distinct from that of *Batophora* and other genera of Dasycladaceae. This morphology has been termed umbrellospore, although it should be considered a highly modified choristospore morphology. The cladospore, choristospore

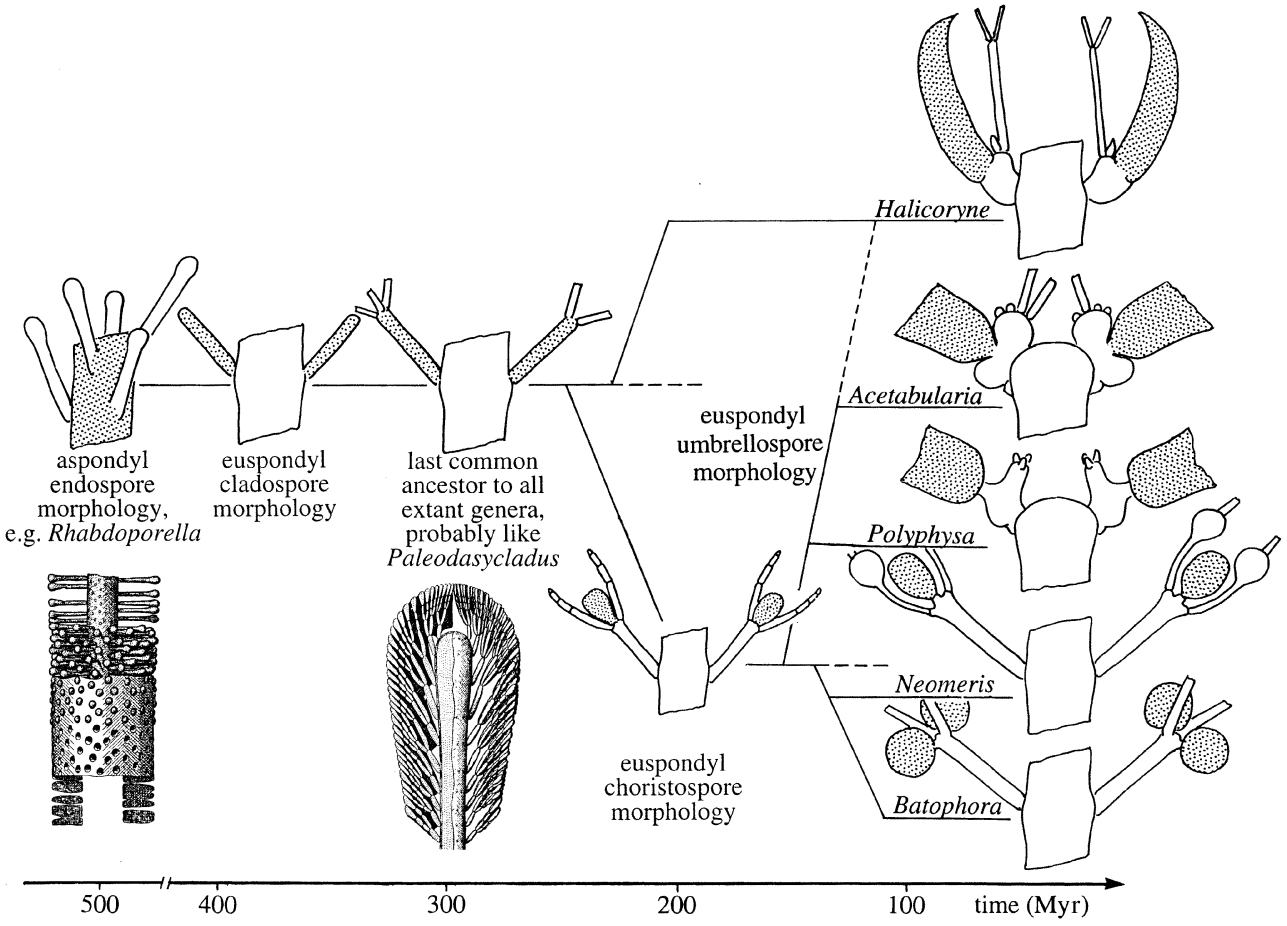

Figure 22. Major evolutionary trends in the evolution of the Dasycladales. The stippled regions indicate the location of the cysts. The exact relationship between *Halicoryne* and other dasycladalean genera remains to be determined. Here, the solid line leading to *Halicoryne* indicates the postulated relationship based on morphogenetic and fossil evidence; the dashed line shows the postulated relationship based on adult morphology. The drawings of fossil dasyclads are from Pia (1927), with permission.

and umbrellospore morphologies are specializations of the vegetative whorl to serve a reproductive function. Therefore, in all extant species the reproductive whorl is homologous to the vegetative whorl.

While there is consensus on the concept that the reproductive whorl is ultimately derived from the vegetative whorl, there is still disagreement regarding the actual correspondence between components of the reproductive and vegetative whorls. Three major homological systems have been presented as solutions to this problem. The first originated from Nägeli's work (1847) and was propounded mainly by Church (1895) (figure 23*a*). He postulated that the cap arose from the 'telescoping' of the main axis. The coronae superior and inferior would be folds of the main axis and the coronal protuberances an aggregate of whorls brought together by an extreme reduction of the interwhorl segments (telescoping). In Church's system, the gametophore is a primary hair segment modified to serve a reproductive function. Solms-Laubach's homological system (1895) is based on his observation of a perforated septum separating the central cavity and the coronal chamber (figure 23*b*). This discovery discredited Nägeli and Church's idea since it became difficult to argue for a continuity between the central cavity and the coronal chamber. Consequently, Solms-Laubach proposed that the coronal chamber and the protuberances of the corona superior are homologous to primary and secondary hair segments, respectively. Because he could not see a clear parallel between the gametophore and any part of the vegetative whorl in *Acetabularia*, he assumed that the gametophore had an independent origin. Valet (1968) put forward a third proposal, where the radial projections of the coronae superior and inferior as well as the gametophore are homologous to secondary hair segments (figure 23*c*). In this case, the protuberances of the corona superior would be equivalent to third-order hair segments. Valet's proposal has been adopted by many contemporary authors (Emberger 1968; Groupe Français d'Étude des Algues Fossiles 1975; Tappan 1980).

These proposals suggest three possible scenarios for the evolution of cladospore forms into choristospore forms and finally into umbrellospore forms. The staging of § 2 leaves no doubt about the correspondence that must be drawn between the coronal chamber and the primary hair segment (see figure 2). Church's idea that the cap represents an aggregate of whorls must therefore be abandoned. The remaining two homological systems depart with respect to the origin of the gametophore and the coronae inferior and superior. These differences will be addressed in § 5(c) and § 5(d).

The lineage presented in figure 22 differs in two ways from recently held ideas on the evolution of the

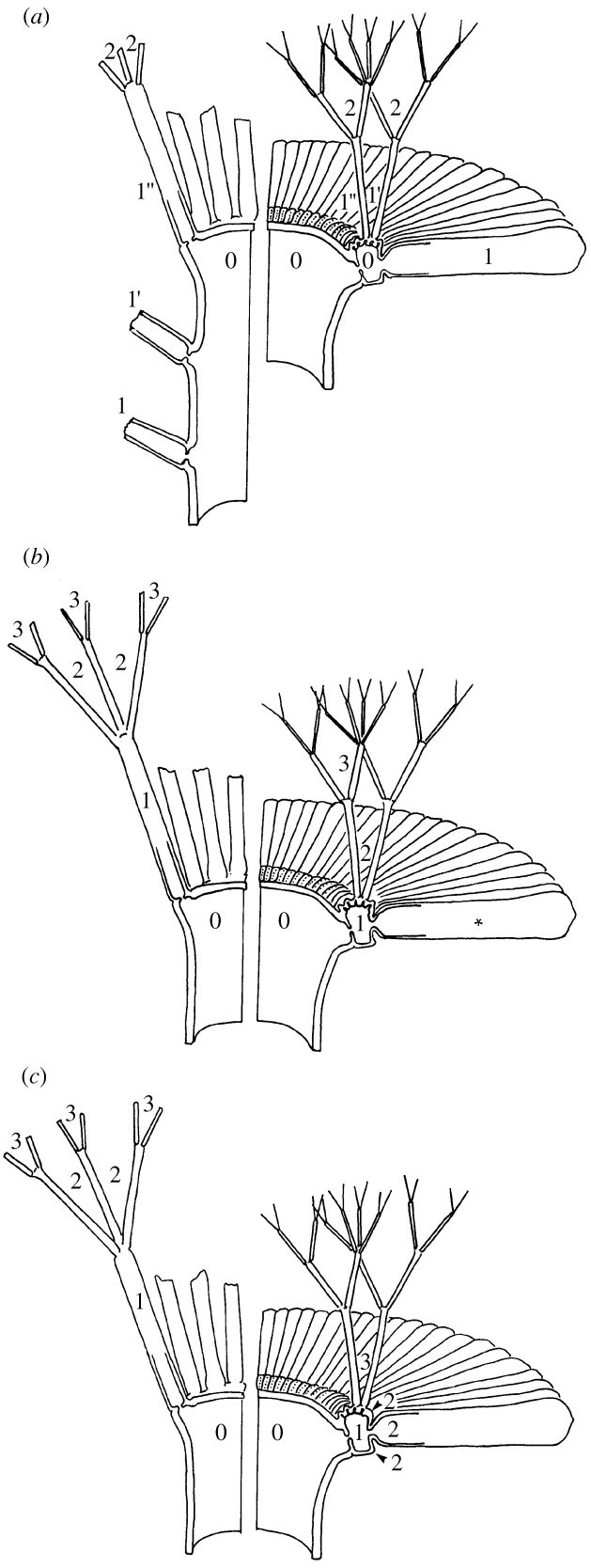

Figure 23. Homology between the vegetative and reproductive whorls of *Acetabularia*. The proposals by (*a*) Church (1895), (*b*) Solms-Laubach (1895) and (*c*) Valet (1968) are presented. The numbers indicate the correspondence between components of the two whorl types. An asterisk denotes a component which has no homologue. For clarity, only two protuberances of the corona superior were represented as fully grown hairs.

Dasycladales. First, we have postulated that the last common ancestor between the Dasycladaceae and the Acetabulariaceae had a choristospore morphology and has therefore occurred relatively recently. We think that the similarity in the morphogenesis of the reproductive structures is strong evidence for this. Moreover, a phylogenetic tree based on ribosomal DNA has provided evidence for a relatively recent ancestor (265 Myr) for the two families (Olsen *et al*. 1994). Second, based on its morphogenesis (§ 2(b)), we have excluded *Halicoryne* from the Acetabulariaceae where it is usually placed. This is to conform with Menzel (1982) who justified the distinction on the basis of the presence of a perforated septum between the coronal chamber and the gametophore. This feature is lacking in other genera of Acetabulariaceae. The exclusion of *Halicoryne* from the Acetabulariaceae is also compatible with the evidence from the fossil record that the genus appeared approximately 205 Myr (Berger & Kaever 1992), that is, very early in the evolution of the Acetabulariaceae and Dasycladaceae. We consider below mechanistic explanations for three major evolutionary advances, namely, the transition from aspondyl to euspondyl forms, the origin of the gametophore, and the origin of the corona inferior.

(b) *Transition from aspondyl to euspondyl forms*

The transition from the aspondyl to the euspondyl morphology was a critical step in the evolution of the dasyclads. How did the simultaneous initiation of appendages in a whorled pattern evolve from the aspondyl morphology where, presumably, appendages were initiated one at a time in a random pattern? At first sight, the transition seems difficult to explain; yet it was repeated in several dasycladalean groups (Pia 1920; Kamptner 1958). A possible explanation emerged from computations using reaction–diffusion mechanisms (Harrison *et al*. 1981, 1988). Whorl patterns do not spring naturally from a single reaction–diffusion system on a hemispherical tip; rather, higher mode solutions produce random patterns reminiscent of the aspondyl morphology. Whorls are formed only if two reaction–diffusion systems are placed in sequence, as in Harrison's model. The first one provides the transition from tip growth to subapical growth (stage 1 to stage 2), the second one breaks the annular region thus formed into a whorl pattern (stage 2 to stage 3). Therefore, the evolutionary advance leading to the transition from aspondyl to euspondyl morphology could have been the intercalation of a new pattern-forming event confining the morphogenesis to an annular region. It is not clear to us how Martynov's buckling model could account for this evolutionary advance. On the other hand, Goodwin (1990) emphasized the fact that a whorled pattern arises naturally, almost ineluctably, from the Goodwin–Trainor equations. Given that the aspondyl morphology preceded the whorled morphology, this feature of the model may need to be reconsidered.

(c) *Origin of the gametophore*

The gametophore has been recognized as a modified hair segment (Emberger 1968; Valet 1968; Tappan 1980) or given an independent origin (Solms-Laubach 1895; Howe 1901; Pia 1920). The first hypothesis is the most parsimonious and the cladospore morphology of certain

fossils represents an appealing intermediate form. However, two observations have led some authors to believe that the gametophore evolved independently. Solms-Laubach's evidence relates to the location of the gametophore (Solms-Laubach 1895). Because the lateral position of the gametophore in *Acetabularia* has no counterpart in the vegetative whorl, Solms-Laubach did not believe in the homology between the gametophore and the vegetative hair. Following the same logic, Solms-Laubach considered the gametophores of *Batophora* and *Dasycladus* to be modified hairs because their location corresponds to the location of secondary hair segments (see figure 6). Solms-Laubach's attitude is in line with the claim that relative position or connection is the most conservative criterion of structural homology (Boyden 1973). Pia (1920) based his view on a different criterion, namely, the lag between the initiation of the gametophore and that of adjacent hairs. This fact was underlined in § 2. The gametophore is initiated several hours (*Acetabularia*) up to several weeks (*Batophora*) after the corresponding hair whorl has appeared. Therefore, in Pia's mind, no matter how close a gametophore could come to occupy the place of a hair segment in a given whorl, the fact that it did not develop concomitantly with the neighbouring hairs was enough to assign it an independent evolutionary origin.

Solms-Laubach's 'spatial argument' and Pia's 'temporal argument' are two sides of an observation previously discussed. In § 2(c) we provided evidence to suggest that the whorl is a unit rather than a collection of individual appendages. If the nature of the whorl in extant species is a good indication of primitive whorls in the Dasycladales, it is hard to argue that in the course of evolution one or a few hairs have been displaced in space and time (of initiation) to serve a reproductive function. In other words, the gametophore cannot be a modified hair simply because the vegetative hairs do not have an existence of their own. Solms-Laubach's homological system preserves the integrity of the whorl by ascribing to the gametophore an independent origin and is, to our minds, to be preferred over the other proposals.

If the gametophore evolved independently, the mechanism responsible for its origin may be different from the mechanism responsible for hair formation. Some observations suggest that they are indeed different. First, the initiation of the gametophore is not, as far as our observations go, preceded by a punctate lysis of the cell wall. Second, the growth of the gametophore is localized near its base rather than at its tip (Serikawa & Mandoli 1998). On the other hand, the reversion of gametophore initials to vegetative growth leading to the differentiation of hairs (figure 9*c*) suggests a certain compatibility between the two mechanisms.

(d) *Origin of the corona inferior*

The radial projections of the corona inferior have been considered to be true lateral organs (Falkenberg 1882; Howe 1901; Valet 1968). Moreover, the presence of a corona inferior has been used as a key taxonomic character within the family Acetabulariaceae (Berger & Kaever 1992). The morphological continuum between the coronal chamber of *Acetabularia* and *Polyphysa* suggests that the projections of the corona inferior do not constitute true appendages. In our view, the origin of the corona inferior is best explained in terms of growth and interference rather than by invoking new pattern-forming events (see the discussion in § 2(b)). A reduction of spacing, a quantitative character, accounts for the qualitative morphological differences between *Polyphysa* and *Acetabularia*. All the models can provide for this transition by assuming change in one of the parameters controlling spacing. For reaction–diffusion, these parameters have either a direct or an indirect genetic basis. For example, simple mutations could provide a morphogenetic protein with a different diffusivity or, more likely, a different rate constant (the D_X, D_Y and a, b, c, d parameters in equation (4)). The modulation of the concentration of a precursor molecule (the [A] and [B] parameters in equation (4)) would have an indirect genetic basis.

6. CONCLUSION

We have defined the 'pattern formation viewpoint' as the practice of identifying pattern-forming events and looking for their mechanisms. Each of the morphogenetic stages we have enumerated involves a pattern-forming event. Among these, probably the most promising for study of possible mechanisms is the formation of the whorl pattern, because it has a parameter, the spacing (λ), which is regulated quantitatively (§ 4(a–c)). This event is associated with several chemical features, e.g. the formation of regularly spaced lytic pits; concentration of actin in the vicinity of these pits (Menzel 1996); and concentration of Ca^{2+}, first in the annular pattern clearly marking the whorl-forming domain, and later in the hair primordia. These features, and especially the quantitative control of λ by Ca^{2+} concentration, point strongly towards a chemical pattern-generating mechanism. The calcium effect has been shown to be consistent with patterning by reaction–diffusion in the cell membrane. It would be interesting if similar tests could be devised for some of the factors in the Goodwin and Trainor mechano-chemical model. These have so far proved elusive. Biochemical identification of the changes, membrane-located and cytoplasmic, that immediately precede wall lysis is clearly needed.

When a definitive identification of the whorl-forming event is reached, will it throw light on development of anything other than the dasyclads? If the answer to this question is positive, the dasyclads may be very helpful because the patterning of their appendages is one of few instances where an extended fossil record is available to document how a specific morphogenetic process has changed with evolution. Some authors (e.g. Church 1919; Chadefaud 1952; Emberger 1968) not only argued for a natural continuity between algae and higher plants, but also emphasized that the algae account for all the major structural innovations in the plant kingdom. This idea had already been recognized for the Dasycladales. The resemblance between the body plan of *Acetabularia* (rhizoid–stalk–hair–cap) and that of higher plants (root–stem–leaf–flower) had been underlined by Nägeli (1847), Church (1895) and Puiseux-Dao (1962, 1965) among others. Solms-Laubach (1895) and Church (1895) drew an even closer parallel between hair and leaf. And more

recently, Mandoli (1998) and Nishimura & Mandoli (1992*a*) have identified juvenile and adult developmental phases in *Acetabularia* closely corresponding to such phases in higher plants. Hagemann (1992) and Kaplan (1992) have also discussed general implications of similar development with and without multicellularity.

These accounts have generally focused on fully developed structures. However, the most striking similarities are seen when one considers the morphogenesis of these structures. In both the dasyclads and higher plants, morphogenesis is a complex instance of apical growth, i.e. tip growth and meristematic growth, respectively. The spatial scale of pattern formation (between 50 and 500 μm) is similar even though the organisms involved may differ in final size by several orders of magnitude. Pattern formation is influenced by the size of the apex, usually in a way suggestive of a wavelength for the pattern: compare *Acetabularia* (Harrison *et al*. 1981), *Equisetum* (Bierhorst 1959) and *Hippuris* (McCully & Dale 1961). For this wide range of genera, the number of laterals in a whorl is proportional to whorl diameter.

We take it as a working hypothesis of the pattern formation viewpoint that a common dynamic is there to be found when examples of morphogenetic processes share so many phenomenological characteristics as do whorl formation in the dasyclads and in higher plants. The fact that the three models described in this paper have their counterparts in higher plants (see, for example, Roberts 1978; Berding *et al*. 1983; Green 1992) indicates that this is a definite possibility.

We are grateful to Dina F. Mandoli (Department of Botany, University of Washington, USA) for providing additional cell lines to test our morphogenetic staging and Audrey Lohachitranont for technical assistance and her sustained interest for this work. The authors would also like to thank Sara Fultz and Peter Ray (Department of Biological Sciences, Stanford University, USA) for their comments on the manuscript. Significant improvements in our writing, particularly in §6, arose from the comments of two anonymous referees whom we wish to thank for their suggestions. This research was supported by NSERC Canada through a postgraduate scholarship to J.D. and an operating grant to L.G.H.

REFERENCES

Adamich, M., Gibor, A. & Sweeney, B. M. 1975 Effects of low nitrogen levels and various nitrogen sources on growth and whorl development in *Acetabularia* (Chlorophyta). *J. Phycol*. **11**, 364–367.

Amtmann, A., Klieber, H. G. & Gradmann, D. 1992 Cytoplasmic free Ca^{2+} in the marine alga *Acetabularia*: measurement with Ca^{2+}-selective microelectrodes and kinetic analysis. *J. Exp. Bot*. **43**, 875–885.

Barattolo, F. 1991 Mesozoic and Cenozoic marine benthic calcareous algae with particular regard to Mesozoic Dasycladales. In *Calcareous algae and stromatolites* (ed. R. Riding), pp. 504–540. Berlin: Springer.

Bary, A. de & Strasburger, E. 1877 *Acetabularia mediterranea*. *Bot. Zeit*. **45**, 713–758.

Berding, C., Harbich, T. & Haken, H. 1983 A pre-pattern formation mechanism for the spiral-type patterns of the sunflower head. *J. Theor. Biol*. **104**, 53–70.

Berger, S. & Kaever, M. J. 1992 *Dasycladales, an illustrated monograph of a fascinating algal order*. Stuttgart, Germany: Georg Thieme.

Bierhorst, D. W. 1959 Symmetry in *Equisetum*. *Am. J. Bot*. **46**, 170–179.

Bonotto, S. 1969 Quelques observations sur les verticilles d'*Acetabularia mediterranea*. *Bull. Soc. R. Bot. Belgique* **102**, 165–179.

Bonotto, S. 1971 Sur un type particulier de morphogenèse anormale chez *Acetabularia crenulata*. *Bull. Soc. R. Bot. Belgique* **104**, 5–12.

Bonotto, S. 1988 Recent progress in research on *Acetabularia* and related Dasycladales. *Prog. Phycol. Res*. **6**, 59–235.

Bonotto, S. 1994 Developmental biology of *Acetabularia*. *J. Mar. Biol. Ass. UK* **74**, 93–106.

Bonotto, S. & Kirchmann, R. 1970 Sur les processus morphogénétiques d'*Acetabularia mediterranea*. *Bull. Soc. R. Bot. Belgique* **103**, 255–272.

Bonotto, S. & Puiseux-Dao, S. 1970 Modification de la morphologie des verticilles et différentiation chez l'*Acetabularia mediterranea*. *C. R. Acad. Sci. Paris* **270**, 1100–1103.

Boyden, A. 1973 *Perspectives in zoology*. Oxford, UK: Pergamon.

Brière, C. 1994 Dynamics of the Goodwin–Trainor mechanochemical model. *Acta Biotheor*. **42**, 137–146.

Chadefaud, M. 1952 La leçon des algues: comment elles ont évolué; comment leur évolution peut éclairer celle des plantes supérieures. *Ann. Biol*. **18**, 9–25.

Church, A. H. 1895 The structure of the thallus of *Neomeris dumetosa*, Lamour. *Ann. Bot*. **9**, 581–608.

Church, A. H. 1919 Thalassiophyta and the subaerial transmigration. *Bot. Memoirs* **3**, 1–95.

Cotton, G. & Vanden Driessche, T. 1987 Identification of calmodulin in *Acetabularia*: its distribution and physiological significance. *J. Cell Sci*. **87**, 337–347.

Cramer, C. 1895 Über *Halicoryne wrightii* Harvey. *Vierteljahrsschrift d. Naturf. Ges. Zürich* **40**, 265–277.

Crawley, J. C. W. 1966 Some observation of the fine structure of the gametes and zygotes of *Acetabularia*. *Planta* **69**, 365–376.

Dao, S. 1957 La gametogenèse chez l'*Acetabularia mediterranea* Lamouroux, Dasycladacée. *C. R. Acad. Sci. Paris* **245**, 1263–1265.

Dumais, J. 1996 Dasycladales morphogenesis: the pattern formation viewpoint. MSc thesis, University of British Columbia, Canada.

Egerod, L. E. 1952 An analysis of the siphonous Chlorophycophyta, with special reference to the Siphonocladales, Siphonales, and Dasycladales of Hawaii. In *University of California publications in botany*, vol. 25 (ed. A. S. Foster, L. Constance & G. F. Papenfuss), pp. 325–454, plates 29–42. Berkeley, CA: University of California Press.

Emberger, L. 1968 *Les plantes fossiles dans leurs rapports avec les végétaux vivants*. Paris: Masson.

Falkenberg, P. 1882 In *Handbüch der Botanik*, vol. 2 (ed. A. Schenk), pp. 269–272. Breslau, Poland: Eduard Trewendt.

Garrill, A., Jackson, S. L., Lew, R. R. & Heath, I. B. 1993 Ion channel activity and tip growth: tip-localized stretch-activated channels generate an essential Ca^{2+} gradient in the oomycete *Saprolegnia ferax*. *Eur. J. Cell Biol*. **60**, 358–365.

Gibor, A. 1973 Observations on the sterile whorls of *Acetabularia*. *Protoplasma* **78**, 195–202.

Gibor, A. 1989 Cellular studies on marine algae. *Int. Rev. Cytol*. **118**, 93–114.

Goodwin, B. C. 1990 Structuralism in biology. *Sci. Progress* **74**, 227–244.

Goodwin, B. C. & Trainor, L. E. H. 1985 Tip and whorl morphogenesis in *Acetabularia* by calcium-regulated strain fields. *J. Theor. Biol*. **117**, 79–106.

PHILOSOPHICAL TRANSACTIONS OF THE ROYAL SOCIETY B BIOLOGICAL SCIENCES

Goodwin, B. C., Skelton, J. L. & Kirk-Bell, S. M. 1983 Control of regeneration and morphogenesis by divalent cations in *Acetabularia mediterranea*. *Planta* **157**, 1–7.

Green, P. B. 1992 Pattern formation in shoots: a likely role for minimal energy configuration of the tunica. *Int. J. Plant Sci.* **153**, 59–75.

Groupe Français d'Étude des Algues Fossiles 1975 Réflexions sur la systématique des Dasycladales fossiles. Étude critique de la terminologie et importance relative des critères de classification. *Géobios* **8**, 259–290.

Hagemann, W. 1992 The relationship of anatomy to morphology in plants: a new theoretical perspective. *Int. J. Plant Sci.* **153**, S38–S48.

Hämmerling, J. 1931 Entwicklung und Formbildungsvermögen von *Acetabularia mediterranea*. *Biol. Zentralbl.* **51**, 633–647.

Harrison, L. G. 1992 Reaction–diffusion theory and intracellular differentiation. *Int. J. Plant Sci.* **153**, S76–S85.

Harrison, L. G. 1993 *Kinetic theory of living pattern*. Developmental and cell biology series, vol. 28. New York: Cambridge University Press.

Harrison, L. G. & Hillier, N. A. 1985 Quantitative control of *Acetabularia* morphogenesis by extracellular calcium: a test of kinetic theory. *J. Theor. Biol.* **114**, 177–192.

Harrison, L. G., Snell, J., Verdi, R., Vogt, D. E., Zeiss, G. D. & Green, B. R. 1981 Hair morphogenesis in *Acetabularia mediterranea* temperature-dependent spacing and models of morphogen waves. *Protoplasma* **106**, 211–221.

Harrison, L. G., Snell, J. & Verdi, R. 1984 Turing's model and pattern adjustment after temperature shock, with application to *Acetabularia* whorls. *J. Theor. Biol.* **106**, 59–78.

Harrison, L. G., Graham, K. T. & Lakowski, B. C. 1988 Calcium localization during *Acetabularia* whorl formation: evidence supporting a two-stage hierarchical mechanism. *Development* **104**, 255–262.

Harrison, L. G., Donaldson, G., Lau, W., Lee, M., Lin, B. P., Lohachitranont, S., Setyawati, I. & Yue, J. 1997 CaEGTA uncompetitively inhibits calcium activation of whorl morphogenesis in *Acetabularia*. *Protoplasma* **196**, 190–196.

Haußer, I., Herth, W. & Reiss, H.-D. 1984 Calmodulin in tip-growing plant cells, visualized by fluorescing calmodulin-binding phenothiazines. *Planta* **162**, 33–39.

Herak, M., Kochansky-Devidé, V. & Gusic, I. 1977 The development of the Dasyclad algae through the ages. In *Fossil algae* (ed. E. Flugel), pp. 143–153. Berlin: Springer.

Howe, M. A. 1901 Observations on the algal genera *Acicularia* and *Acetabulum*. *Bull. Torrey Bot. Club* **28**, 321–334.

Kamptner, E. 1958 Über das System und die Stammesgeschichte der Dasycladaceen (*Siphoneae verticillatae*). *Ann. Naturhist. Mus. Wien* **62**, 95–122.

Kaplan, D. R. 1992 The relationship of cells to organisms in plants: problem and implications of an organismal perspective. *Int. J. Plant Sci.* **153**, S28–S37.

Kellner, G. & Werz, G. 1969 Die Feinstruktur des Augenfleckes bei *Acetabularia*—Gameten und sein Verhalten nach der Gametenfusion. *Protoplasma* **67**, 117–120.

Knight, M. R., Knight, H. & Watkins, N. J. 1995 Calcium and the generation of plant form. *Phil. Trans. R. Soc. Lond.* B **350**, 83–86.

Kof, É. M., Filichkina, O. A. & Kefeli, V. I. 1987 Histological features of structural organization of the regenerating *Acetabularia* cell wall. *Soviet J. Dev. Biol.* **18**, 333–339.

Kratz, R. F., Young, P. A. & Mandoli, D. F. 1998 Timing and light regulation of apical morphogenesis during reproductive development in wild-type populations of *Acetabularia acetabulum* (Chlorophyceae). *J. Phycol.* **34**, 138–146.

Lacalli, T. C. 1981 Dissipative structures and morphogenetic pattern in unicellular algae. *Phil. Trans. R. Soc. Lond.* B **294**, 547–588.

Lü, H. & McLaughlin, D. J. 1991 Ultrastructure of the septal pore apparatus and early septum initiation in *Auricularia auricula-judae*. *Mycologia* **83**, 322–334.

McCully, M. E. & Dale, H. M. 1961 Variations in leaf number in *Hippuris*. A study of whorled phyllotaxis. *Can. J. Bot.* **39**, 611–625.

Mandoli, D. F. 1996 Establishing and maintaining the body of *Acetabularia acetabulum* in the absence of cellularization. *Semin. Cell Dev. Biol.* **7**, 891–901.

Mandoli, D. F. 1998 Elaboration of body plan and phase change during development of *Acetabularia*: how is the complex architecture of a giant unicell built? *A. Rev. Plant Physiol. Plant Mol. Biol.* **49**, 173–198.

Martynov, L. A. 1973 Optical mechanical properties and deformation of the cell membrane of *Acetabularia*. *Biophysics* **18**, 999–1003.

Martynov, L. A. 1975 A morphogenetic mechanism involving instability of initial form. *J. Theor. Biol.* **52**, 471–480.

Martynov, L. A. 1976 Number of verticils and umbel rays in *Acetabularia*. *Soviet J. Dev. Biol.* **7**, 147–155.

Maynard Smith, J. 1968 *Mathematical ideas in biology*. Cambridge University Press.

Menzel, D. 1980 Plug formation and peroxidase accumulation in two orders of siphonous green algae (Caulerpales and Dasycladales) in relation to fertilization and injury. *Phycologia* **19**, 37–48.

Menzel, D. 1982 Peroxidase in Siphonalen Grünalgen. Vergleich ende cytologische und cytochemische Untersuchungen über ihre Beteiligung an der Wundreaktion und Pfropfbildung. PhD thesis, Freien Universität, Berlin, Germany.

Menzel, D. 1994 Tansley review no. 77. Cell differentiation and the cytoskeleton in *Acetabularia*. *New Phytol.* **128**, 369–393.

Menzel, D. 1996 The role of the cytoskeleton in polarity and morphogenesis of algal cells. *Curr. Opin. Cell Biol.* **8**, 38–42.

Menzel, D. & Elsner-Menzel, C. 1989 Maintenance and dynamic changes of cytoplasmic organization controlled by cytoskeletal assemblies in *Acetabularia* (*Chlorophyceae*). In *Algae as experimental systems*, plant biology series, vol. 7 (ed. A. W. Coleman, L. J. Goff & J. Stein-Taylor), pp. 71–91. New York: Alan R. Liss.

Menzel, D. & Elsner-Menzel, C. 1990 The microtubule cytoskeleton in developing cysts of the green alga *Acetabularia*: involvement in cell wall differentiation. *Protoplasma* **157**, 52–63.

Nägeli, C. 1847 *Die neuern Algensysteme*. Zürich, Switzerland: Schulthess.

Nishimura, N. J. & Mandoli, D. F. 1992*a* Vegetative growth of *Acetabularia acetabulum* (Chlorophyta): structural evidence for juvenile and adult phases in development. *J. Phycol.* **28**, 669–677.

Nishimura, N. J. & Mandoli, D. F. 1992*b* Population analysis of reproductive cell structure of *Acetabularia acetabulum* (Chlorophyta). *Phycologia* **31**, 351–358.

Okamura, K. (ed.) 1907–1909 *Icones of Japanese algae*, vol. 1, pp. 217–221, plate 43. Tokyo: Kazamashobo.

Olsen, J., Stam, W. T., Berger, S. & Menzel, D. 1994 18S rDNA and evolution in the Dasycladales (Chlorophyta): modern living fossils. *J. Phycol.* **30**, 729–744.

Orlovich, D. A. & Ashford, A. E. 1994 Structure and development of the dolipore septum in *Pisolithus tinctorius*. *Protoplasma* **178**, 66–80.

Oster, G. F. & Odell, G. M. 1984 The mechanochemistry of cytogels. *Physica* D **12**, 333–350.

Pia, J. 1920 Die *Siphoneae verticillatae* von Karbon bis zur Kreide. *Abhandl. Zool-Botan. Ges. Wien* **11**, 1–263.

Pia, J. 1923 Einige Ergebnisse neuerer Untersuchungen über die Geschichte der *Siphoneae verticillatae*. *Z. Indukt. Abstammungs-Vererbungslehre* **30**, 63–98.

Pia, J. 1927 Thallophyta. In *Handbüch der Paläobotanik*, vol. 1 (ed. M. Hirmer), pp. 31–136. Munich and Berlin: R. Oldenbourg.

Poethig, R. S. 1990 Phase change and the regulation of shoot morphogenesis in plants. *Science* **250**, 923–930.

Prigogine, I. & Lefever, R. 1968 Symmetry-breaking instabilities in dissipative systems, II. *J. Chem. Phys.* **48**, 1695–1700.

Puiseux-Dao, S. 1962 Recherches biologiques et physiologiques sur quelques Dasycladacées, en particulier, le *Batophora oerstedii* et *l' Acetabularia mediterranea* Lam. *Rev. Gen. Bot.* **69**, 409–503.

Puiseux-Dao, S. 1965 Morphologie et morphogenèse chez les Dasycladacées. In *Travaux de biologie végétale dédiés au Professeur Plantefol*, pp. 147–170. Paris: Masson.

Puiseux-Dao, S. 1972 *Acetabularia and cell biology.* London: Logos Press.

Reiss, H.-D. & Herth, W. 1979 Calcium gradients in tip growing plant cell visualized by chlorotetracycline fluorescence. *Planta* **146**, 615–621.

Roberts, D. W. 1978 The origin of Fibonacci phyllotaxis—an analysis of Adler's contact pressure model and Mitchison's expanding apex model. *J. Theor. Biol.* **74**, 217–233.

Schmid, R., Idziak, E-M & Tünnermann, M. 1987 Action spectrum of the blue-light-dependent morphogenesis of hair whorls in *Acetabularia mediterranea*. *Planta* **171**, 96–103.

Schweiger, H. G., Berger, S., Kloppstech, K., Apel, K. & Schweiger, M. 1974 Some fine structural and biochemical features of *Acetabularia major* (Chlorophyta, Dasycladaceae) grown in the laboratory. *Phycologia* **13**, 11–20.

Serikawa, K. A. & Mandoli, D. F. 1998 An analysis of morphogenesis of the reproductive whorl of *Acetabularia acetabulum*. *Planta* **207**, 96–104.

Sievers, A. & Schnepf, E. 1981 Morphogenesis and polarity of tubular cells with tip growth. In *Cytomorphogenesis in plants*. Cell biology monographs, vol. 8 (ed. O. Kiermayer), pp. 265–299. Vienna, Austria: Springer.

Solms-Laubach, H. Graf zu. 1895 Monograph of the Acetabularieae. *Trans. Linn. Soc. Lond. 2* (*Botany*) **5**, 1–39.

Svedelius, N. 1923 Zur Kenntnis der Gattung *Neomeris*. *Svensk Botanisk Tidskrift*. **17**, 449–471.

Tappan, H. 1980 *The paleobiology of plant protists*. San Francisco, CA: Freeman.

Tepfer, M. & Taylor, I. E. P. 1981 The interaction of divalent cations with pectic substances and their influence on acid-induced cell wall loosening. *Can. J. Bot.* **59**, 1522–1525.

Timoshenko, S. & Woinowsky-Krieger, S. 1959 *Theory of plates and shells*. New York: McGraw-Hill.

Trewavas, A. & Knight, M. 1994 Mechanical signalling, calcium and plant form. *Plant Mol. Biol.* **26**, 1329–1341.

Turing, A. M. 1952 The chemical basis of morphogenesis. *Phil. Trans. R. Soc. Lond.* B **237**, 37–72.

Valet, G. 1968 Contribution a l'étude des Dasycladales. I. Morphogenèse. *Nova Hedwigia* **16**, 21–82, plates 4–26.

Vanden Driessche, T. 1990 Calcium as a second messenger in *Acetabularia*: calmodulin and signal transduction pathways. In *Calcium as an intracellular messenger in eucaryotic microbes* (ed. D. H. O'Day), pp. 278–300. Washington, DC: American Society for Microbiology.

Vanden Driessche, T., Petiau-de Vries, G. M. & Guisset, J.-L. 1997 Tansley review no. 91. Differentiation, growth and morphogenesis: *Acetabularia* as a model system. *New Phytol.* **135**, 1–20.

Werz, G. 1959 Über polare Plasmaunterschiede bei *Acetabularia*. *Planta* **53**, 502–521.

Werz, G. 1965 Determination and realization of morphogenesis in *Acetabularia*. *Brookhaven Symp. Biol.* **18**, 185–203.

Werz, G. 1968 Plasmatische Formbildung als Voraussetzung für die Zellwandbildung bei der Morphogenese von *Acetabularia*. *Protoplasma* **65**, 81–96.

Woronine, M. 1862 Sur les algues marines *Acetabularia* Lamx. et *Espera* Dcne. *Ann. Sci. Nat. 4* (*Botanique*) **16**, 200–214, plates 5–11.

Zar, J. H. 1984 *Biostatistical analysis*. Englewood Cliffs, NJ: Prentice-Hall.

Zeller, A. & Mandoli, D. F. 1993 Growth of *Acetabularia acetabulum* (Dasycladales, Chlorophyta) on solid substrata at specific cell densities. *Phycologia* **32**, 136–142.

PHILOSOPHICAL TRANSACTIONS OF THE ROYAL SOCIETY B BIOLOGICAL SCIENCES